DEVELOPMENT OF A LOW-COST ASEISMIC BASE ISOLATION DEVICE FOR PROTECTION OF STRUCTURAL SYSTEMS FROM DAMAGING EFFECTS OF EARTHQUAKES

by

Mustafa Gökhan KESTİ

B.Sc. in Civil Engineering, Istanbul Kültür University, 2005

Submitted to the Kandilli Observatory and
Earthquake Research Institute in partial fulfillment of
the requirements for the degree of
Master of Science

Graduate Program in Earthquake Engineering
Boğaziçi University
2009

DEVELOPMENT OF A LOW-COST ASEISMIC BASE ISOLATION DEVICE FOR PROTECTION OF STRUCTURAL SYSTEMS FROM DAMAGING EFFECTS OF EARTHQUAKES

APPROVED BY:

Prof. Dr. Mustafa Ö. ERDİK (Thesis Supervisor)	…….
Prof. Dr. Erdal ŞAFAK	……
Assoc. Prof. Dr. Oğuz ÖZEL (İstanbul University)	……

DATE OF APPROVAL: 17.04.2009

ACKNOWLEDGEMENTS

I would like to express my great appreciation and gratitude to my thesis supervisor Professor Dr. Mustafa Ö. ERDİK, for spending his invaluable time, sharing his experience, his vision to improve this study and considerable effects in the completion of the study.

I must offer my thanks to Professor Dr. Eser DURUKAL for her valuable suggestions. I would also like to express my thanks to Assist. Prof. Dr. Waiel MOWRTAGE for sending his valuable time during the tests.

I also want to express special thanks to Assist Prof. Dr. Gülüm TANIRCAN and my colleagues, Dr. Cüneyt TÜZÜN, Dr. Göktürk ÖNEM, Ph.D. Student Yavuz KAYA for their support and assistance in my thesis study.

I must also express and state special thanks to Oktay ÇIRAĞ and Ahmet KORKMAZ who spent their invaluable time and energy with me during the test.

I also want to state my pleasure to ULUS YAPI an Eren KALAFAT for providing and manufacturing BNC devices.

Finally, I have to thank my parents Fikri KESTİ and Sema KESTİ for their endless support, patience and continuous encouragement. In contrary, this study is dedicated to them.

ABSTRACT

DEVELOPMENT OF A LOW-COST ASEISMIC BASE ISOLATION DEVICE FOR PROTECTION OF STRUCTURAL SYSTEMS FROM DAMAGING EFFECTS OF EARTHQUAKES

Due to the killing thousands of people in the twentieth century and seismicity of our country, earthquakes are one of the most important natural hazards for our country. Therefore the earthquake resistance of structural system plays central role for earthquake protection. This M.Sc. thesis research's concern is to illustrate some base isolation techniques and to propose a base isolation device to improve the earthquake resistance of structural systems. The so-called Ball-N-Cone (BNC) aseismic base isolation device is experimentally studied and results are given.

ÖZET

DÜŞÜK MALİYETLİ TABAN YALITIM SİSTEMİNİN GELİŞTİRİLMESİ

Ülkemizin yüksek deprem riski altında olması ve yirminci yüzyılda binlerce kişinin deprem sonrası ölümü sebebiyle, depremler ülkemiz açısından en önemli doğal afetlerden biridir. Bu sebeple depreme dayanıklı yapı tasarımı, yapıların depremden korunmasında çok önemli rol oynamaktadır. Bu yüksek lisans tez çalışmasının amacı daha önce yapılmış olan taban izolasyon sistemlerini göstererek, yeni bir taban izolasyon sistemini önermektir. Ball-N-Cone (BNC) diye anılan sismik izolasyon sistemi deneysel olarak incelenmiş ve elde edilen sonuçlar sunulmuştur.

TABLE OF CONTENTS

Page

LIST OF FIGURES

LIST OF TABLES

Page

1. GENERAL VIEW OF ASEISMIC BASE ISOLATION TECHNIQUE

Throughout the history, earthquakes are one of the most important natural hazards in human life. The overwhelming majority of deaths and injuries in earthquakes occur because of the collapse of buildings; and much of the economic loss and social disruption caused by earthquakes is equally attributable to the failure and other man-made structures. Therefore, earthquakes and the damage they have caused become the most important aspect for civil engineers. Hence, innovative techniques have been developed to protect the structures from damaging effects of earthquakes. Engineering techniques for modifying the structure to achieve better earthquake resistance are available, and can be expected to become more widely used in the future.

1.1. Aseismic Base Isolation Technique

Conventionally, seismic design of building structures which plays a central role in earthquake protection is based on the concept of increasing the resistance capacity of the structures against earthquakes by employing, for example, the use of shear walls, braced frames, or moment-resistant frames. However, these traditional methods often result in high floor accelerations for stiff buildings, or large interstory drifts for flexible buildings. Because of this, the building contents and nonstructural components may suffer significant damage during a major earthquake, even if the structure itself remains basically intact. This is not tolerable for buildings whose contents are more costly and valuable than the buildings themselves. High-precision production factories are one example of buildings that contain extremely costly and sensitive equipment. Additionally, hospitals, police and fire stations, and telecommunication centers are examples of facilities that contain valuable equipment and should remain operational immediately after an earthquake.

Many mechanisms, invented over the past century to protect a building from the damaging effects of an earthquake for not only minimizing interstory drifts, but also reducing floor accelerations by using some type of support that uncouples the structures from the ground. Several ideas which allows the structure to slide were proposed referred to as *aseismic base isolation.* The early examples are Sevastopol, Crimea, and a five-story school in Mexico City, Mexico that built on rollers, as well as one building in China which has a sand layer between the foundation and the building. Now, widely accepted in earthquake-prone regions of the world for protecting structures from strong ground motion, recent examples of base-isolated construction include structures in Armenia, Chile, China, Indonesia, Italy, Japan, New Zealand, the United States, Turkey and Uzbekistan.

Base isolation has also been referred to as passive control, as the control of structural motion is not exercised through a logically driven external agency, but rather through a specially designed interface at the structural base or within the structure, which can reduce or filter out the forces transmitted from the ground.

The principle of base isolation is quite simple. Reducing the earthquake forces transmitted to the building by introducing some form of the flexible support. That means these forces are much lower transmitted to the structure than the fixed base structures. In addition to this, it can be applied not only to the structures, but also to any equipment or museum displays in buildings by installation between the base of equipment or museum displays and the supporting floor.

Despite wide variation in detail, the concept of seismic base isolation which follows two basic approaches with certain common features is quite simple. In the first approach the isolation reduces the effect of the horizontal components of the ground acceleration by interposing structural elements with relatively low horizontal (lateral) stiffness, but high vertical stiffness, between the structure and the foundation. This gives the structure a fundamental frequency that is much lower than both its fixed-base frequency and the predominant frequencies of the ground motion. In other words, the isolation system introduces a layer of low horizontal stiffness between the structure and the foundation. With this isolation layer the structure has a natural period that is much longer than its

fixed-base natural period. This lengthening of period can reduce the pseudo acceleration thereby the earthquake-induced forces in the structure, but the deformation is increased; this deformation is concentrated in the isolation system, however, accompanied by only small deformations in the structure. The first dynamic mode of the isolated structure involves deformation only in the isolation system, the structure above being, for all intents and purposes, rigid. The higher modes producing deformation in the structure are orthogonal to the first mode and, consequently, to the ground motion. The higher modes do not participate in the motion, so that if there is high energy in the ground motion at these higher frequencies, this energy cannot be transmitted into the structure. The isolation system does not absorb the earthquake energy, but deflects it through the dynamics of the system. Although a certain level of damping is beneficial to suppress any possible resonance at the isolation frequency, the concept of isolation does not depend on damping. In fact, excessive damping can reduce the effectiveness of the isolation system by acting as a conduit for energy to be induced in the higher modes of the isolated structure.

The most common system of this type which is known as the elastomeric bearing as well as a laminated rubber bearing (Figure 1.1) uses short, cylindrical bearings with one or more holes and alternating multilayered laminated hard rubber bearings with layers of reinforcing steel plates as the load-carrying component of the system. Because of the reinforcing steel plates, this type of bearings are very strong and stiff enough to sustain vertical loads, yet are soft and sufficiently flexible under lateral forces (Figure 1.2), thereby reducing the demand on it and producing the isolation effect. Furthermore, this ability to deform horizontally enables the bearing to reduce significantly the shear forces induced by the earthquake. While the major function of elastomeric bearings is to reduce the transmission of shear forces to the superstructure through lengthening of the vibration period of the entire system, they should provide sufficient rigidity under the service load levels and minor earthquakes. In reality, the reduction in seismic forces transmitted to the superstructure through installation of laminated rubber bearings is achieved at the expense of large relative displacements across the bearings. If substantial damping can be introduced into the bearings or the isolation system, bearing with inclusion of a central lead plug has been devised (Figure 1.3). In other words, since natural damping of the rubber is low, additional damping is usually provided by some form of mechanical damper. These have included lead plugs inserted into the holes, also as shown in Figure

1.4, hydraulic dampers, steel bars, or steel coils. Metallic dampers provide energy dissipation through yielding, thus reducing nonlinearity in the system. The bearing displacements are controlled by use of either damping-enhanced rubber or by the use of additional energy dissipating elements, known as dampers or energy absorbers, such as mild steel dampers, lead plugs in the bearings, frictional elements, or viscous damping devices. These bearings are easy to manufacture, have no moving parts, are unaffected by time, and resist environmental degradation.

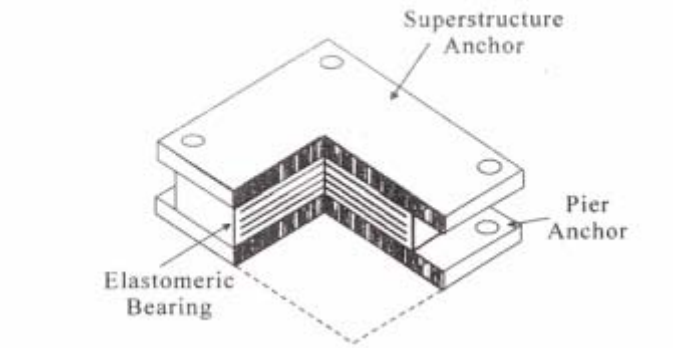

Figure 1.1 Elastomeric Bearing [Kelly, 2004]

Figure 1.2 Deformed laminated rubber bearing (Courtesy of I.D. Aiken) [Chopra, 2001]

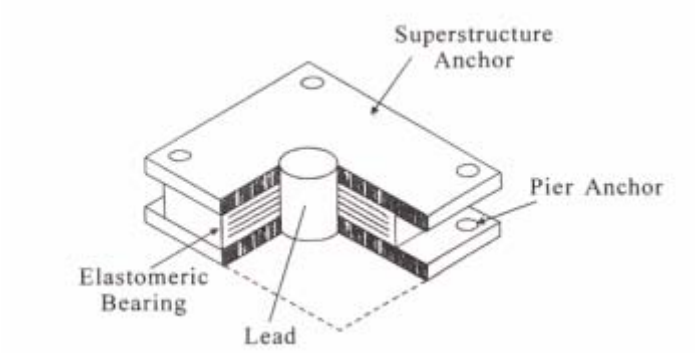

Figure 1.3 Laminated rubber bearing with lead core [Kelly, 2004]

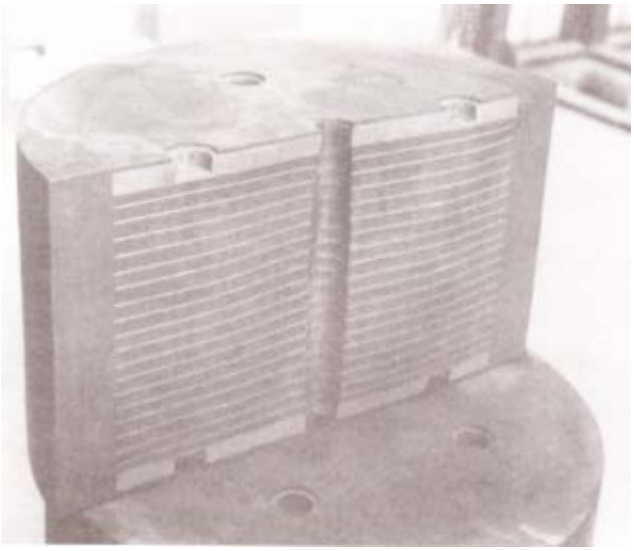

Figure 1.4 Section of a laminated rubber bearing (Courtesy of I.D. Aiken) [Chopra, 2001]

In the second approach, the isolation system uses sliding elements between the foundation and the base of the structure. In other words, this approach increses flexibility in a structure is to provide a *sliding* or *friction surface* between the foundation and the base of the structure. It assumes that the shear force transmitted to the superstructure across the isolation interface is limited by the static friction force, which equals the product of the coefficient of friction, keeping as low as practical, and the weight of the superstructure. In other words, a low level of friction will limit the transfer of shear across the isolation interface – the lower the coefficient friction, the lesser the shear transmitted. Nevertheless, it must be sufficiently high to provide a friction force that can sustain strong

winds and small earthquakes without sliding, a requirement that reduces the isolation effect. Indeed, a fairly high value of frictional coefficient is needed. Many frictional surfaces have sliding characteristics sensitive to pressure and to the relative velocity of slip; because the slip process is intrinsically nonlinear, a proper dynamic analysis must also be nonlinear. Furthermore, any sudden change in the stiffness of the overall structure when slipping or sticking occurs has the effect of generating high-frequency vibrations in the structure – vibrations at frequencies that might not be present in the ground motion. The system responds by transforming low-frequency energy in the ground motion into high-frequency energy in the structure.

There is no effective restoring force is an another problem with using sliders – and only sliders – in an isolation system thus, the code requirements for the displacement are extremely large. Because this displacement can be in any horizontal direction, the diameter of the bearing plates and the support system must be very large. In addition, the superstructure components bearing on the isolators must be designed for large moments caused by these large displacements. Shortly, a sliding structure is the residual displacements that occur after major earthquakes.

There are several ways to introduce a restoring force capability to remedy this problem. The sliding displacements are controlled by high-tension springs or laminated rubber bearings, or by making sliding surface curved - concave – so as to provide a restoring – recentering – force, otherwise unavailable in this type of system, to return the structure to its equilibrium position. This is the idea behind the most popular frictional device, the so-called *Friction Pendulum System* (FPS), which utilizes a spherical concave surface – as shown in Figure 1.5 – and where the weight of the structure is carried on spherical sliding surfaces that slide relative to each other when the ground motion exceeds a threshold level. As it is mentioned before, to guarantee that sliding structure can return to its original position, other mechanisms, such as high-tension springs and elastomeric bearings, can be used as an auxiliary system to generate the restoring forces. Furthermore, the restoring action is, known as recentering action, caused by raising the building slightly when sliding occurs on the spherical surface. Developed in 1986 (Zayas et al., 1987), this system was first used to retrofit a four-story apartment building in San Francisco badly damaged in the 1989 Loma Prieta, California, earthquake. The retrofit involved installing

a steel-moment resisting frame at ground level that supports the upper three floors of a wood-framed structure. Isolators were placed under the columns of the steel frame.

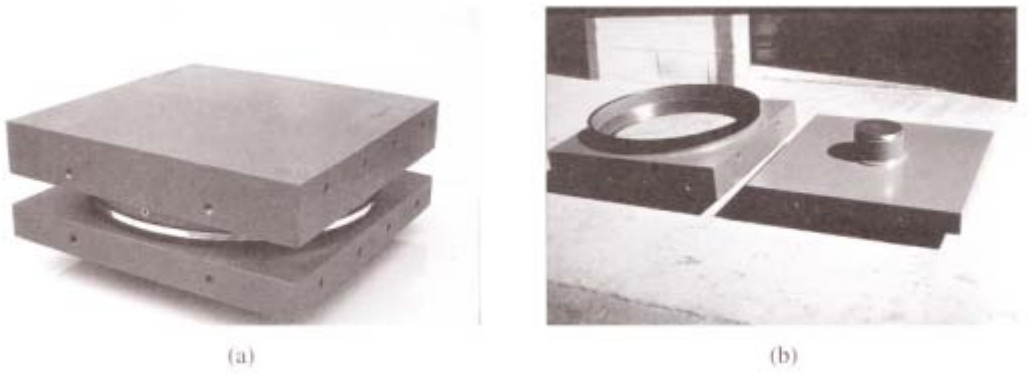

Figure 1.5 (a) Friction pendulum sliding bearing; (b) internal components (Countesy of V.A. Zayas) [Chopra, 2001]

1.2. Some Applications of Aseismic Base Isolation Technique in Turkey

Earthquakes caused serious threads for human lives and economies. Because of 21,000 heavily damaged or collapsed building during the 1999 Kocaeli earthquake, the earthquake resistance become more important issue for Turkey. During the earthquakes significant damages occurred in the superstructures and the contents of the infrastructures. Therefore, retrofit of damaged structures become important aspect. Aseismic base isolation of structures is a mature technology of mitigation of seismic damage for civil structures and equipment, and has proven to be reliable and cost-effective for many structures. The applications of seismic isolation to structures in Turkey is only recent. The current list structures with seismic isolation are as follows;

- ✓ Egegaz LNG Storage Tanks
- ✓ İstanbul-Atatürk Airport Terminal (Retrofit)
- ✓ Bolu Viaducts
- ✓ Kocaeli Hospital
- ✓ Tarabya Hotel (Retrofit)
- ✓ Erzurum State Hospital (Under Construction)
- ✓ Antalya Airport Terminal (Retrofit)

- ✓ Ankara Congress and Trade Center (Under Construction)
- ✓ T.E.B. Headquarters (Design Ready)
- ✓ Gülburnu Bridge (Under Construction)

2. LOW – COST SEISMIC ISOLATION

2.1. Introduction

The recent earthquakes have again showed that the majority of deaths and injuries happens when the earthquakes occur. That means earthquake resistant design is the most important aspect for civil engineers which I mentioned before. Aseismic base isolation is a good solution for protection of structural systems from damaging effects of earthquakes. In contrast, the weight and cost of isolators are problematic for adopting. In addition, it can't be usable for housing. To solve this problem the *low-cost aseismic base isolation systems* become more important issue. Many studies have already done in this concept.

2.2. Thermal Expansion Bridge Bearings as Seismic Isolators

Thermal expansion bridge bearings were studied by Kelly and Konstantinidis in 2007. Their suggestion is in contrast to seismic bearings thermal expansion bridge bearings are much less expensive. The primary weight in an isolator is due to steel reinforcing plates, which are used to provide the vertical stiffness of the rubber-steel composite element. The in-service demands on these bearings are, of course, much lower, but the tests reported herein have shown that even if displacements of seismic-demand magnitude are applied to them they can deform without damage. The primary reason for this is the fact that the top and bottom surfaces can roll off the support surfaces and no tension stresses are produced. The unbalanced moments are resisted by the vertical load through offset of the force resultants on the top and bottom surfaces (Figure 2.2.1).

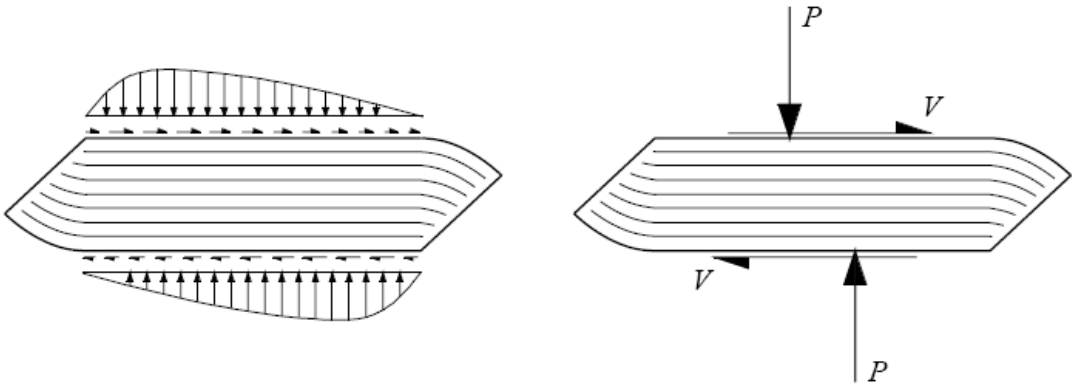

Figure 2.2.1 *Left*: Normal and shear stress distributions on the top and bottom faces of the unbonded bearing in its deformed shape. *Right*: The moment created by the offset of the resultant compressive loads, *P*, balances the moment created by the shear, *V*. [Kelly and Konstantinidis, 2007]

They tested the bearings and survived very large shear strains comparable to those expected of conventional seismic isolators under seismic loading. Their purpose of research is to suggest that both the weight and the cost of isolators can be reduced by using thinner steel reinforcing plates, no end-plates and no bonding to the support surfaces. Since the demands on the bonding to the thin reinforcing plates are reduced, a simpler and less expensive manufacturing process can be used.

2.3. Rolling-ball Isolation System

2.3.1. Introduction

The second type which is colled “Rolling-Ball Isolation System” was studied by Guerreiro, Azevedo and Muhr in 2007. It had been developed at TARRC [Tun Abdul Razak Research Centre] which is suitable for light structures that are less than 10t [Cook et al. 1997; Muhr et al., 1997]. The system is simple. Steel balls rolling on rubber tracks, to bear the load and to provide damping, and rubber springs to provide a self-centring capability (Figure 2.3.1). Two images of a real device are also displayed, corresponding to undeformed (in fact, in the case shown, lateral displacement is prevented by transportation plates, still in situ) and deformed layouts.

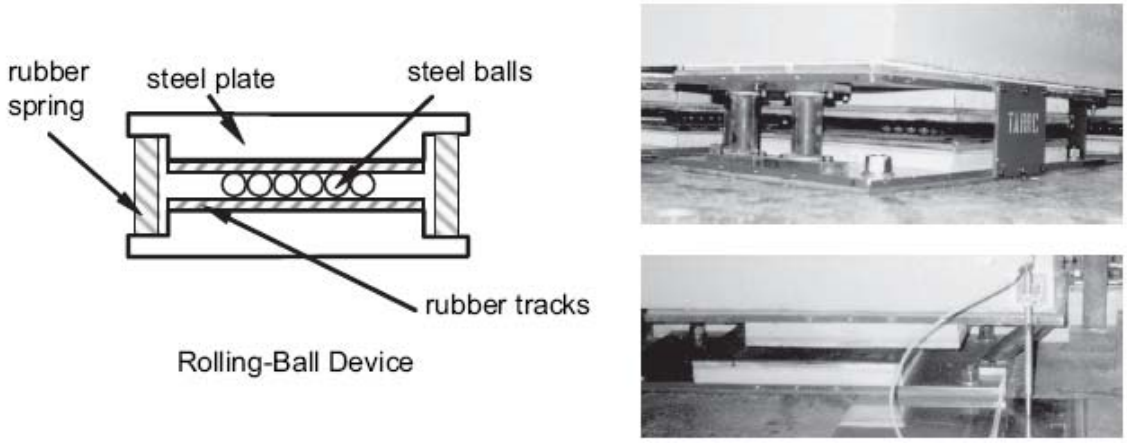

Figure 2.3.1 Rolling Ball Device [Guerreiro et.al, 2007]

It follows that the rolling ball isolation system is most suited to light structures with a low ratio of height of centre of mass to base width, or for which it would not be acceptable for the isolators to permit rocking or vertical modes. Examples of such structures include light electrical devices, light structures used as stands for sensitive equipment, museum pieces of art and, in general, any kind of equipment that is simultaneously light and sensitive to ground motion." [Guerreiro et al., 2007]

2.3.2. Experimental Studies

"The rolling-ball system has been partially evaluated in previous projects involving shaking- table tests, as indicated in Table 2.3.1.

The Projects mentioned in Table 2.3.1 permitted only rather limited testing. A new Project (ECOEST 2) provided an opportunity to try a low damping soft system that had not previously been tried, as well as to carry out carefully chosen variations of stiffness, damping, excitation and structure flexibility." [Guerreiro et al., 2007]

TABLE 2.3.1 Previous shaking-table studies of rolling-ball isolation system [Guerreiro et.al., 2007]

Project	Type of tests	Tracks	Springs	Superstructure
EERC [Foti & Kelly, 1996]	monoaxial	high damping	steel coil, soft	flexible model building
ENEL/ISMES/TARRC collaboration [Bergamo et al., Part I, 2005]	monoaxial	high damping	steel coil, soft	flexible model building
REEDS [Bergamo et al. Part II, 2005]	triaxial	low damping	rubber, stiff	flexible electrical structure

2.3.2.1. Testing Scheme : "A model structure was devised, and made at ISMES, based on two rectangular slabs of concrete, fixed together using M16 studding (Figure 2.3.2). In this way, the natural scale structure was devised to have a fixed mass but an adjustable stiffness associated with the top degree of freedom in the horizontal plane. The length of the studs could be adjusted to obtain an appropriate natural frequency for the fixed-base superstructure. Including fixtures (notably the transducers, the top plates of the isolators and the studs), the mass of the base slab was 945 kg and the mass of the top slab was 575 kg. Artefacts (maximum 8 kg in total) were placed on the table and on the two levels of the isolated structure to provide a visual perception of the intensity of the shaking and of its frequency content. Insofar as their mass is insignificant compared to that of the slabs, their key parameters are natural frequency and ratio of height of centre of mass to width of base, neither of which depend on scale.

The position of the isolators under the structure is shown in plan view in Figure 2.3.2B; they were bolted down to appropriate threaded holes in the shaking-table (pitched at 300 mm), and upwards to studs anchored in the lower concrete slab. Note that in the photograph the isolators are partially dismantled, so that both top and bottom rubber tracks, and the array of balls between them, can be seen." [Guerreiro et al., 2007]

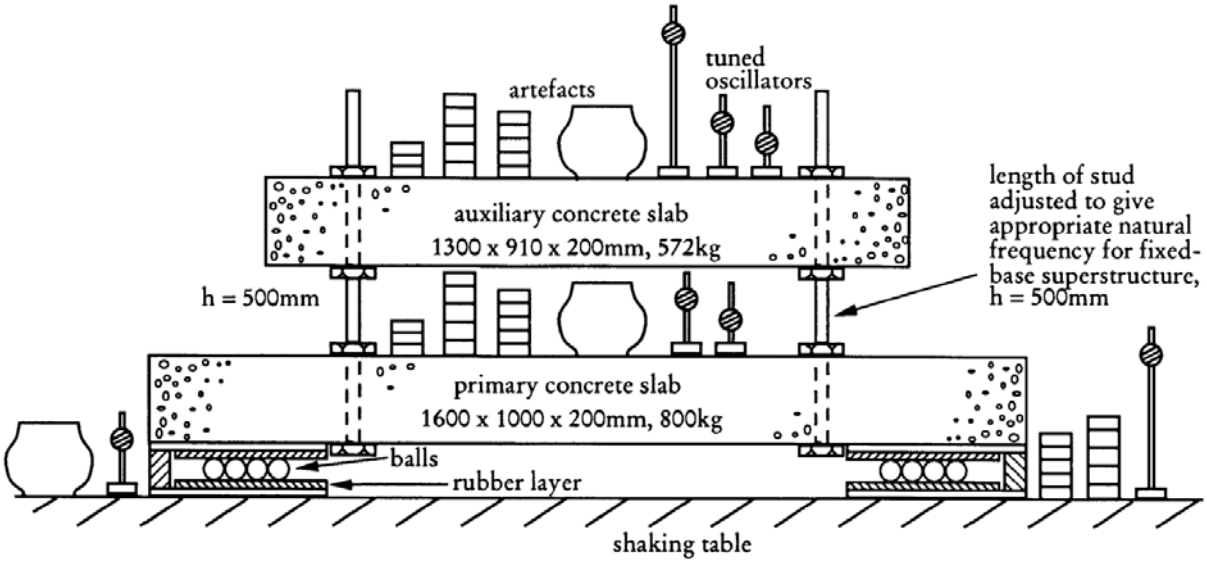

Figure 2.3.2a Lateral view of testing scheme

[Guerreiro et al., 2007]

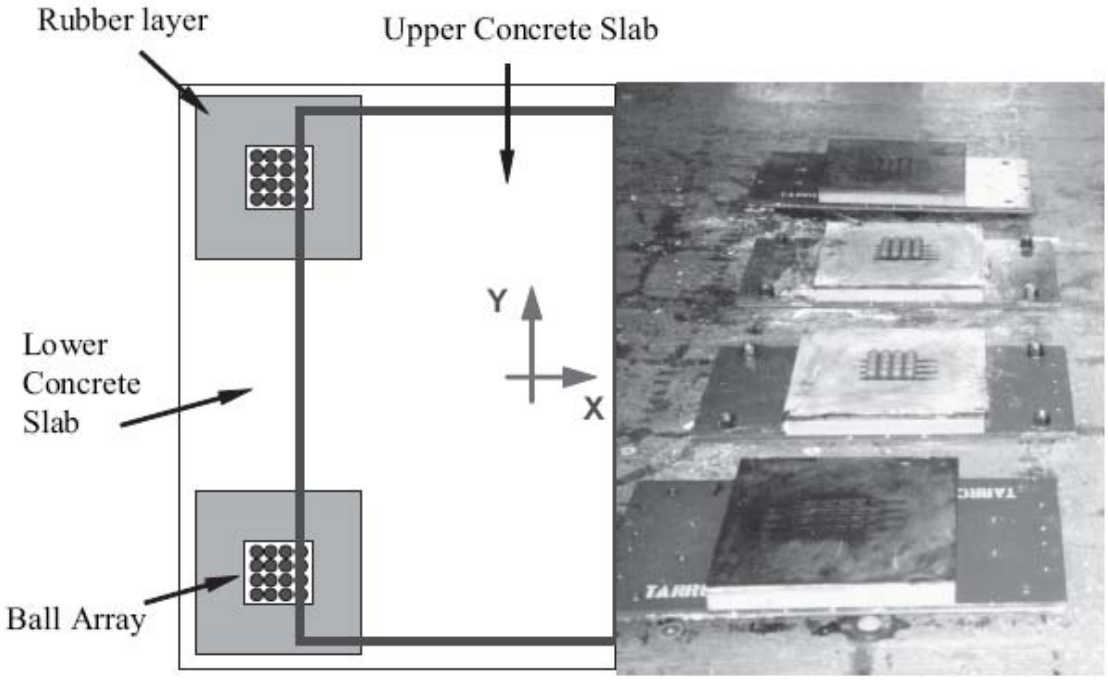

Figure 2.3.2b Plan view and image of the isolators beneath structure

[Guerreiro et al., 2007]

Table 2.3.2 displays, also for the two materials, results of some miscellaneous standard tests.

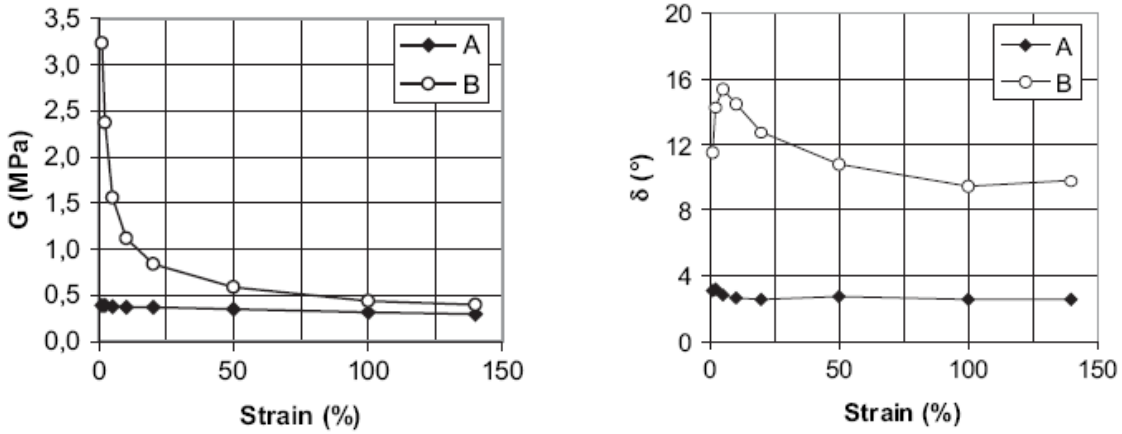

Figure 2.3.3 Dynamic shear properties of rubber compounds A and B — influence of strain level at 1 Hz frequency. [Guerreiro et al., 2007]

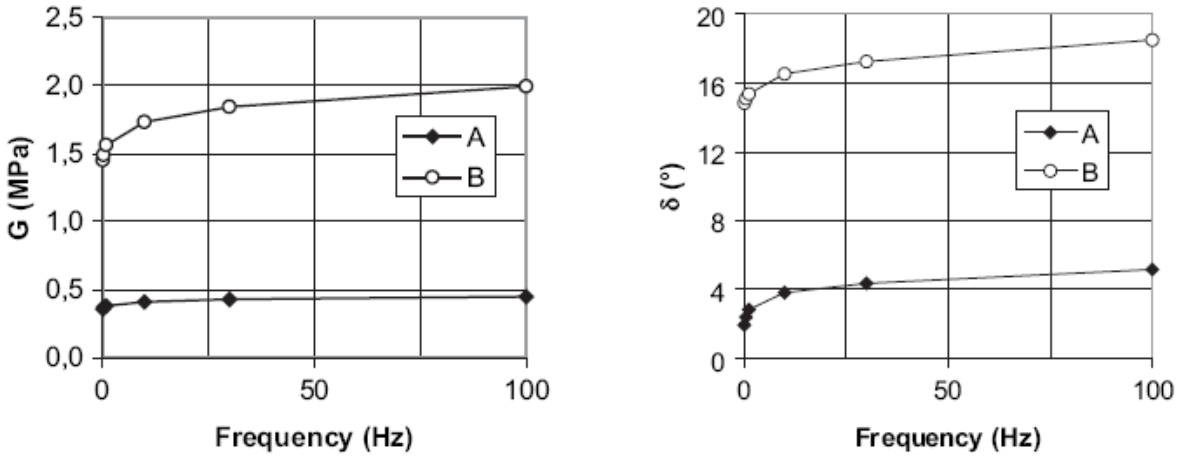

Figure 2.3.4 Dynamic shear properties of rubber compounds A and B — influence of frequency for a 5% strain**.** [Guerreiro et al., 2007]

They noticed that compound A (low damping) exhibits G and loss factor values which are independent of the input strain level, while, for the B compound, G and δ^0 depend on strain amplitude, typical of filled rubber. As expected, the loss factor values are consistently higher for the B compound, while its G values are substantially higher in the lower range of the imposed strain values. Both the G and loss factor values are not very

sensitive to the frequency content of the motion although a slight increase in both values can be observed, for both compounds, with the increase of frequency. The rubber springs depicted in Figure 2.3.1 were cylinders of rubber 80 mm long bonded to steel endplates. They were moulded from rubber compound A in three different diameters: 30, 40, or 50 mm. In principle, it was possible to fix up to 3 cylindrical rubber springs at each end of each isolator. However, in practice, a set of 4 springs — one for each outer end of each isolator — was the most ever used in the tests; all four springs had the same diameter, either 30 or 50 mm.

The sequence of 35 tests carried out on the Master shaking-table at ISMES consisted of the analysis of different layouts which included variations in the location of the top mass, isolation system characteristics (tracks and springs) and different excitation time histories; in addition, each excitation was run at several amplitudes.

Two different configurations for the model structure were analyzed. In the first configuration, designated “Mass Down”, the top mass was rigidly attached to the bottom one; in the second (“Mass Up”), the top mass was linked to the bottom one by means of the four M16 steel studs, the separation between the upper face of the lower mass and the lower face of the upper mass being 500 mm (Figure 2.3.5). The first configuration corresponds to a rigid structure attached to the isolation system, while the second to a structure with a frequency ≈2.5 Hz on the top of the isolation system.

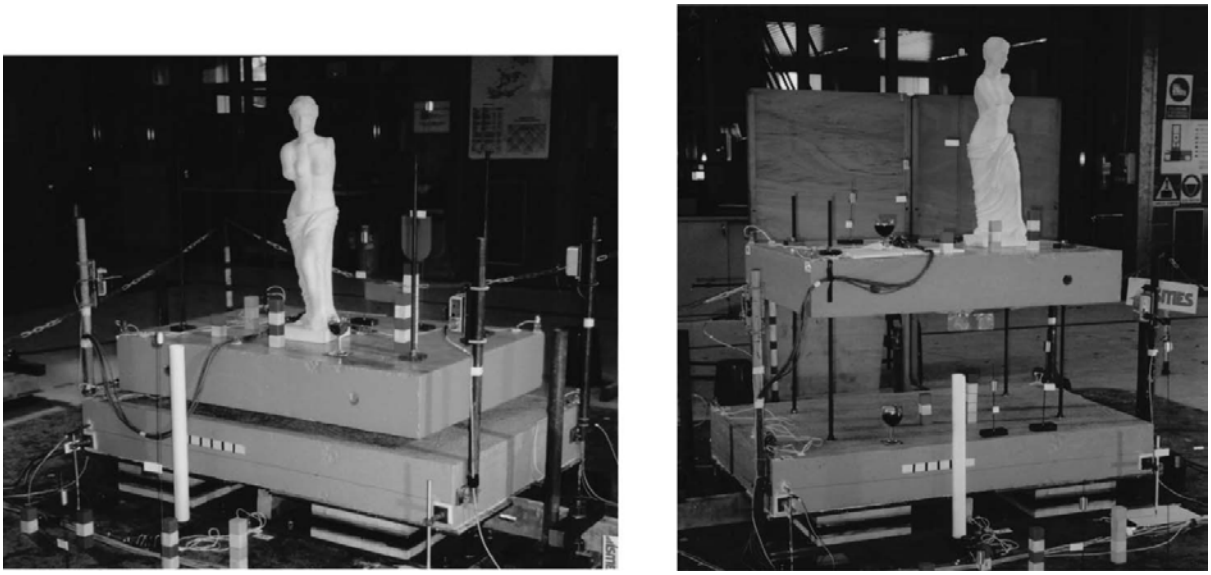

Figure 2.3.5 View of two test set-ups with Mass Down (left) and Mass Up (right). [Guerreiro et al., 2007]

2.3.3. Testing, Results and Conclusion

"The results shows that the use of this system is highly effective in reducing the damaging effects of an earthquake. Two different rubber springs $(\phi 30 \text{ and } \phi 50)$ were tested in a double shear configuration under six different ground motions. The effect of no spring was also tried. All records were applied as uniaxial tests. Biaxial tests were also carried out.

The performance of any isolation system can be evaluated by means of the acceleration response of the isolated structure and its relationship with the ground acceleration. For the analysis of the results of the shaking table test, and to allow further studies involving different motions and different system characteristics, a single degree of freedom model with a special element for the simulation of the Rolling Ball (RB) system behavior has been developed.

The RB element consists of a parallel association of three elements, each one representing a different phenomenon:

• the participation of the rubber spring;
• the rolling resistance of the balls on the rubber tracks;
• the memory effects of the rubber track surface indentation due to the ball pressure.

The modular nature of the system enables it to be designed to meet a wide range of horizontal stiffness and damping requirements, or load capacities, but it is intrinsically most suited to light structures.

Results of an experimental campaign of shaking-table tests show that there is usually an effective reduction of the acceleration levels induced in structures isolated with such devices, while maintaining the response displacements within acceptable values.

For flexible structures, the interstory drifts are generally substantially smaller than the ones that could be observed in non-isolated systems.

The experimental campaign also enabled the assessment of the main characteristics of the isolation devices, allowing the evaluation of the values of the most important parameters that characterize the seismic response of such devices.

A numerical model was developed to simulate the seismic response of any kind of structure isolated with the rolling ball system. Results are shows that numerical simulations and experimental results are same." [Guerreiro et al., 2007]

2.4. Roller Type Isolation Device For Houses

2.4.1. Introduction

The third study on a low-cost aseismic base isolation is "Roller type isolation device for houses" by Ueda, Fujita, Iiba and Enomoto in 2005.

2.4.2. Construction

"Roller type isolation device consists of rail having circular-linear combined 1st and 2nd stiffness, wheel and axles and plane bearing with PTFE coating. X-Y rail motion mechanism enable to absorb impact of horizontal X-Y direction when acceleration applied by earthquake by pendulum motion with friction between axles and bearing. After earthquake wheel will return to center of rail by restoring force. Figure 2.4.1 shows circular-linear combined shape of rail. Here T shows natural period of the system, r_1 is radius of circular rail, k_1 is spring constant (1st stiffness), P_v is vertical load, Q_d is breaking load, d is diameter of axle, D is diameter of wheel, μ is friction coefficient of bearing and θ is inclination of linear rail. 1 shows top plate, 2 shows wheelframe, 3 as base plate, 4 as wheel, 5 as bearing, 6 as axles and 7 shows rail. Natural period of system, 1st and 2nd stiffness, break load and friction coefficient can be determined by (2.4.1)～(2.4.3) formula [Ueda et al., 2005]."

$$T = 2\pi\sqrt{r_1 / g} \tag{2.4.1}$$

$$k_1 = \frac{P_v}{r_1} \tag{2.4.2}$$

$$Q_d = P_v \cdot \mu \tag{2.4.3}$$

$$\mu = \left(\frac{d}{D}\right) \cdot \mu_0 \tag{2.4.4}$$

$$\ddot{x}_{cl} = x_c \cdot \omega_0^2 \tag{2.4.5}$$

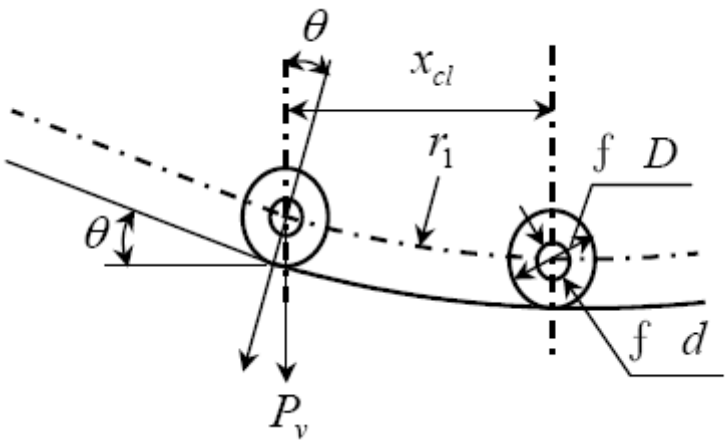

Figure 2.4.1 Circular-linear combined shape of rail
[Ueda et al., 2005]

2.4.3. Shaking Table Test

Model house (Figure 2.4.2) is used with roller type devices (Figure 2.4.3). The device is designed to have approximately 4 sets natural period at circular and inclined rail part which though vary to it's amplitude. μ is the friction coefficient which is between roller and axle is designed as 3% which almost independent to the load. Allowable amplitude in any direction is designed as ±250 mm. 4 sets of this device are inserted to support 2715 kg model house. Below house, steel frame with H-shape beam is combined. (Shown in Figure 2.4.3).

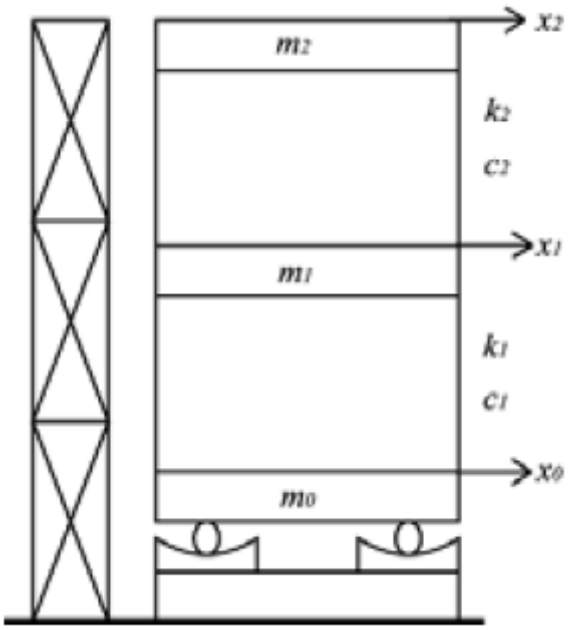

Figure 2.4.2 Analysis model
[Ueda et al., 2005]

Figure 2.4.3 Test model house
[Ueda et al., 2005]

Statistic load test with appropriate weight has been conducted to determine friction coefficient and performance of the system. Friction coefficient has been calculated from measured horizontal load, deflection and vertical load. Here coefficient is calculated using bellow formula (2.4.6). Inclination of strait part of rail is calculated using bellow formula (2.4.7).

$$\mu = \left(F1_{ave} - F2_{ave}\right) \Big/ 2 \tag{2.4.6}$$

$$\theta = \left(F1_{ave} + F2_{ave}\right) \Big/ 2 \tag{2.4.7}$$

Equations of motion of the model are expressed in three phases, as shown below, considering transition of static/dynamic friction due to the presence or absence of sliding at the rolling friction damper.

Phase 1 (no rolling friction)

$$x_0 = \text{constant} \tag{2.4.8}$$

$$\dot{x}_0 = 0 \tag{2.4.9}$$

$$\ddot{x}_0 = 0 \tag{2.4.10}$$

$$m_1\ddot{x}_1 + c_1\dot{x}_1 + c_2\left(\dot{x}_1 - \dot{x}_2\right) + k_1x_1 + k_2\left(x_1 - x_2\right) = -m_1\ddot{z} \tag{2.4.11}$$

$$m_2\ddot{x}_2 + c_2\left(\dot{x}_2 - \dot{x}_1\right) + k_2\left(x_2 - x_1\right) = -m_2\ddot{z} \tag{2.4.12}$$

Phase 2 (rolling at 1st stiffness)

$$m_0\ddot{x}_0 + c_0\dot{x}_0 + c_1\left(\dot{x}_0 - \dot{x}_1\right) + k_0x_0 + k_1\left(x_0 - x_1\right) + \mu\cdot\left(m_0 + m_1 + m_2\right)\cdot g\cdot\operatorname{sgn}\left(\dot{x}_0\right) = -m_0\ddot{z} \tag{2.4.13}$$

$$m_1\ddot{x}_1 + c_1\left(\dot{x}_1 - \dot{x}_0\right) + c_2\left(\dot{x}_1 - \dot{x}_2\right) + k_1\left(x_1 - x_0\right) + k_2\left(x_1 - x_2\right) = -m_1\ddot{z} \tag{2.4.14}$$

$$m_2\ddot{x}_2 + c_2\left(\dot{x}_2 - \dot{x}_1\right) + k_2\left(x_2 - x_1\right) = -m_2\ddot{z} \tag{2.4.15}$$

Phase 3 (rolling at 2nd stiffness)

$$\begin{aligned} &m_0\ddot{x}_0 + c_0\dot{x}_0 + c_1\left(\dot{x}_0 - \dot{x}_1\right) + k_1\left(x_0 - x_1\right) + \left\{x_{cl}k_0 + k_s\left(\left|x_0\right| - x_{cl}\right)\right\}\operatorname{sgn}\left(x_0\right) + \ldots \\ &\ldots + \mu\cdot\left(m_0 + m_1 + m_2\right)\cdot g\cdot\operatorname{sgn}\left(\dot{x}_0\right) = -m_0\ddot{z} \end{aligned} \tag{2.4.16}$$

$$m_1\ddot{x}_1 + c_1\left(\dot{x}_1 - \dot{x}_0\right) + c_2\left(\dot{x}_1 - \dot{x}_2\right) + k_1\left(x_1 - x_0\right) + k_2\left(x_1 - x_2\right) = -m_1\ddot{z} \tag{2.4.17}$$

$$m_2\ddot{x}_2 + c_2\left(\dot{x}_2 - \dot{x}_1\right) + k_2\left(x_2 - x_1\right) = -m_2\ddot{z} \tag{2.4.18}$$

The transition criteria Phase 1, Phase 2 and Phase 3 are:

From Phase 1 to Phase 2

$$\begin{aligned} &\left|k_0x_0 + m_0\ddot{z}\right| > \mu\cdot\left(m_0 + m_1 + m_2\right)\cdot g \\ &\left|x_0\right| > x_{cl} \end{aligned} \tag{2.4.19}$$

From Phase 1 to Phase 3

$$\left|x_{cl}k_0 + k_s\left(\left|x_0\right| - x_{cl}\right) + m_0\ddot{z}\right| > \mu\cdot\left(m_0 + m_1 + m_2\right)\cdot g$$
$$\left|x_0\right| > x_{cl} \tag{2.4.20}$$

From Phase 2 to Phase 1

$$\left|m_0\ddot{z}\right| < 2\cdot\mu\cdot\left(m_0 + m_1 + m_2\right)\cdot g$$
$$\dot{x}_0 = 0 \tag{2.4.21}$$

From Phase 2 to Phase 3

$$\left|x_0\right| > x_{cl} \tag{2.4.22}$$

From Phase 3 to Phase 1

$$\left|m_0\ddot{z}\right| < 2\cdot\mu\cdot\left(m_0 + m_1 + m_2\right)\cdot g$$
$$\dot{x}_0 = 0 \tag{2.4.23}$$

From Phase 3 to Phase 2

$$\left|x_0\right| < x_{cl} \tag{2.4.24}$$

4th accuracy Runge-Kutta-Gill method has been used for digital analysis of this equation.

2.4.4 Conclusion

Shaking table tests results showing good performance and confirming analytical model.

2.5. Theoretical and Experimental Study on A Base Isolation System Using Roller Bearings

2.5.1. Introduction

Another base isolation system with roller bearings has been studied by Xiangyun, Xuehai, Qingmin, Dingguo and Qianfeng. The system is simple and convenient to apply. Not only can it effectively control the earthquake action conveyed to superstructure and the displacement of that superstructure, but it can also automatically restore the building to its original place. Based on the references (Diyuan, Wangqingmin, Fengdingguo, 1992, LinYing, 1990) this paper reports theoretical analysis and testing research on a base isolation system with roller bearings. Simultaneously, seismic response of superstructure has been analyzed with the computer program of time history analysis. The result shows that the theoretical analysis is identical with testing value.

2.5.2. Theory Investigation of Rigid Body Model

A spherical ball rollers, which are constrained to roll between spherical housings as shown in Figure 2.5.1 was used in this study. There are lower housings set in the top of the foundation and upper housings set in the underside of the superstructure. The system provides enhanced lateral stiffness and an automatic restoring capability. Suitable designs of the housing and rollers radius are needed to provide the required characteristics.

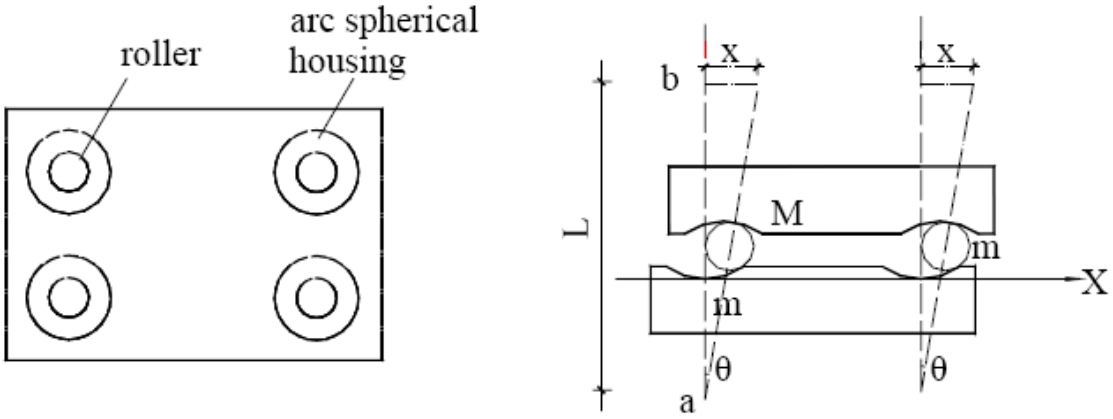

a) Plan b) Cross-section

Figure 2.5.1 Computation model of rigid body

[Xiangyun et al.]

2.5.3. Equation of motion

"The calculation model of rigid body is shown in Figure 2.5.1. *R* is radius of the spherical housing and *r* is the radius of the roller. Assuming touching surface between roller and housing is rough enough, the roller simply rolls without relative slip. Form LaGrange equation: $\frac{d}{dt}\left(\frac{\partial T}{\partial \theta}\right)-\frac{\partial T}{\partial \theta}+\frac{\partial V}{\partial \theta}=Q_\theta$, The motion differential equation of rigid body, that is:

$$\left(M+\frac{7}{20}m\right)L\frac{1}{\cos\theta}\ddot{\theta}+\left(Mg+\frac{1}{2}mg+M\ddot{u}_v\right)tg\theta+\frac{F}{\cos\theta}=-M\ddot{u}_0 \tag{2.5.1}$$

Where θ is general coordinates, F is rolling friction, $F=\mathrm{sgn}\left(\dot{x}\right)\frac{\delta}{r}Mg$ (δ is coefficient of damping roller, *r* is radius of roller), $L=2\left(R-r\right)$, $\ddot{u}_0$ is acceleration excited horizontally, $\ddot{u}_v$ is acceleration excited vertically. Since the mass of roller (*m*) is smaller than the mass of superstructure (*M*), stiffness (*k*) can be neglected in calculation. In seismic design, the influence of the vertical acceleration of the ground is not considered.

The value of θ is generally smaller than 5^0 in vibration, hence: $\cos\theta = 1$, $tg\theta = 1$, $x = L\sin\theta = L\theta$, and the equation can be simplified to:

$$M\ddot{x} + \frac{Mg}{L}x = -\mathrm{sgn}(\dot{x})\frac{\delta}{r}Mg - M\ddot{u}_0 \tag{2.5.2}$$

Equation 2.5.1 is the differential equation of motion of the superstructure, simplified as a rigid body, due to the effects of the base isolation system. The restoring force is $p = \frac{Mg}{L}x$, and the fundamental frequency is $\omega_0 = \sqrt{\frac{g}{L}}$. If a resilient damping device is set up as a layer of the base isolation, and assuming that *k* is a base isolation stiffness coefficient, and *c* is the damping coefficient, the motion equation is"

$$M\ddot{x} + c\dot{x} + kx = -\mathrm{sgn}(\dot{x})\frac{\delta}{r}Mg - M\ddot{u}_0 \tag{2.5.3}$$

2.5.4. Conclusions

1. The computation model and equation of motion of base isolation system with roller bearings has been established. Theoretical analysis corresponded fairly well with test results. Simultaneously, it has been proved that a rolling base isolation system has good base isolation properties. A theoretical foundation for studying more deeply has been proposed.

2. Analysis verified that a rolling base isolation system response can provide artificial control in an earthquake action. It is not influenced by peak excitation acceleration, and the response spectrum of the acceleration does not vary with natural period of structure basically.

3. Spherical housings provide the building's motion a restoring force and a base isolation system possessing the ability to automatically restore. The restoring force varies with the mass of the structure. The greater the mass of the structure, the larger restoring force is.

4. The theoretical optimum stiffness of the isolation layer has been presented. For a typical shear structure (natural period of vibration $T_0 = 0.2 \sim 0.3s$), we can choose an optimum stiffness, i.e. $T_{or} = 2.0 \sim 3.0s$. [Xiangyun et.al., 2003]."

3. THE BNC (BALL-N-CONE) ISOLATION SYSTEM

3.1. Introduction

In this section we will try to review the development of a seismic isolation bearing called Ball-N-Cone (BNC) bearing. The principles of operation of the BNC bearing have been established by Zoltan and Szidarovszky (1995). Herein, we state these principles and provide a complete description of the behavior of the bearing.

The BNC bearing (cross sectional view shown in Figure 3.1) is gravity restoring type of device consisting of two conical plates, which holds a ball in between. During an earthquake the ball moves along the two concave conical surfaces, causing the supported mass to rise, with motions equivalent to those of a simple pendulum. In BNC isolation system the geometry of the isolation bearings and the gravity is used to achieve the desired seismic-isolation results. During the rise along the conical surface the bearing develops a lateral resisting force that is equal to the gravity-induced restoring force. Independent of the displacement, for small φ angles the lateral force is equal to:

$$F = \varphi \cdot W \tag{3.1}$$

Where φ, is the cone slope and W is the supported weight. The first advantage of the above feature is that the lateral force is directly proportional to the supported weight. This causes the center of stiffness and lateral resistance of the bearing group to coincide directly with the center of mass of the supported system, hence compensating for mass eccentricities. This property minimizes adverse torsional motions of the supported structure. A second advantage is that the output seismic force is physically limited, regardless of the seismic displacement, which is restored by gravity.

The BNC's rolling friction, in other words its damping, is negligible. The BNC devices are often employed in parallel with viscous or friction dampers to reduce its seismic displacement and consequently its size. lts cone apex is often rounded for smooth response without impact and for effects such as temperature movement.

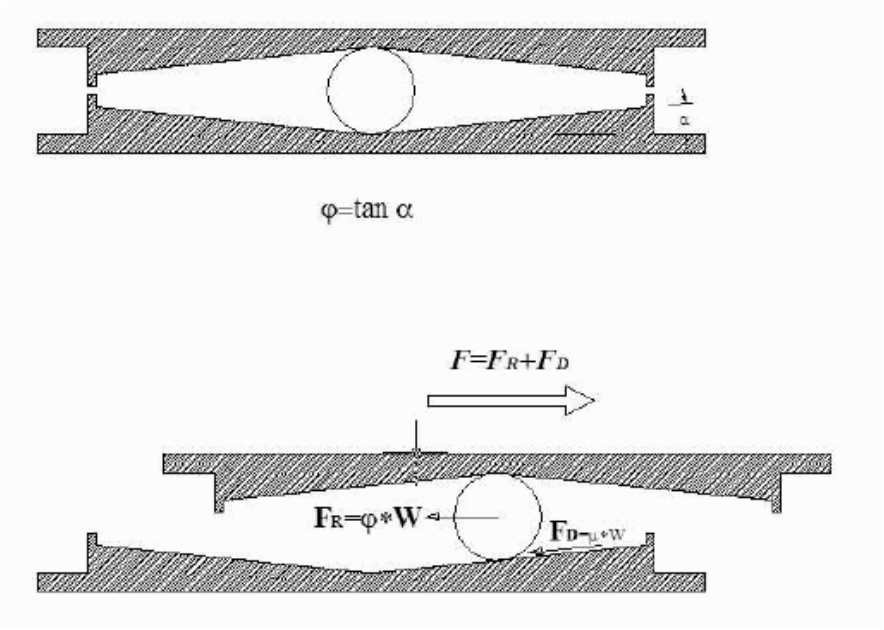

Figure 3.1 Cross sectional view of BNC

3.2. Advantages of BNC

- Ball in Cone response is not weight dependent. It can prevent rocking.
- Gravity restoring force provides recentering of the system.
- Ball in Cone also use for art object's and museum displays. It is quite small in plan. It will not interfere with the art object's view.
- Ball in cone bearings have no natural period. Resonance is impossible for the system isolated with ball in cone devices.
- Equivalent pendulum length double limits the acceleration
- Low-cost production.
- Easy implementation.

3.3. Theory

There are three different type of cone shapes (shown in Figure 3.2) which are considered in order to deal with linear, bilinear, and Heaviside gravity restoring. Linear restoring is achieved by a spherical plate surface (shown in Figure 3.3) (path C) while Heaviside restoring is proper for conical surfaces. However it is practical to round the cone apex. When the cone apex radius is smaller than the ball radius path A), the BNC would rattle, and the restoring law would be discontinuous. When it is larger than the ball radius (path B), bilinear restoring law will be generated. And when it is equal to the dish radius (path C), the restoring law would be linear.

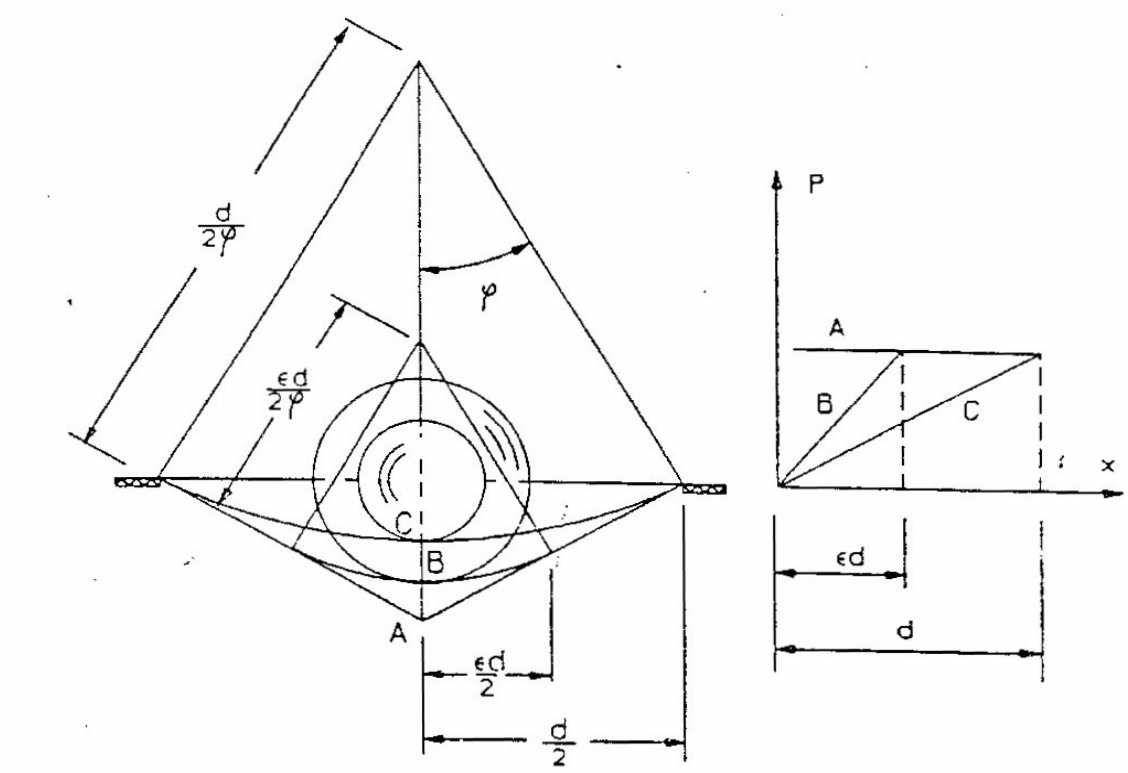

Figure 3.2 BNC geometries and corresponding restoring laws

The behavior of the system is investigated for three different cone apexes. The first one consists of two-rounded cone (path C). The motion and responses are linear.

3.3.1. Path C Response

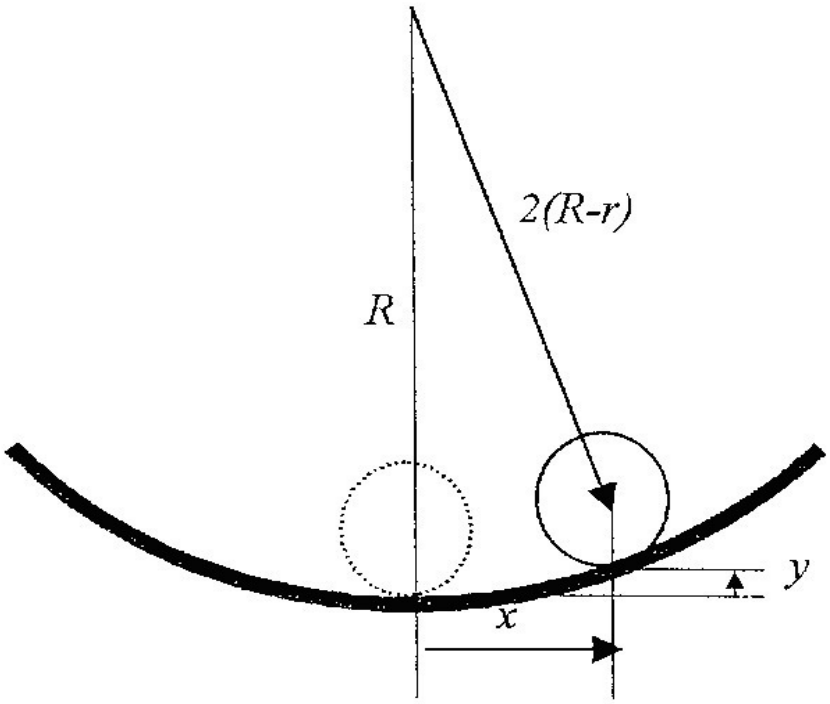

Figure 3.3 BNC Geometry

$$x = 2(R - r)\sin\varphi \tag{3.2}$$

$$y = 2(R - r)(1 - \cos\varphi) \tag{3.3}$$

$$\tan\varphi = \frac{x}{\sqrt{4 - (R - r)^2 - x^2}} \tag{3.4}$$

For small φ

$$\tan\varphi = \frac{x}{2(R-r)} \tag{3.5}$$

Assume the ground motion is in the form

$$\ddot{x}_g = x_0 \cdot \omega^2 \cdot \sin(\omega t) \tag{3.6}$$

Forces acting on the system and equation of motion can be written as

$$m\ddot{x} - mg \cdot \tan\varphi = m\ddot{x}_g \tag{3.7}$$

$$m\ddot{x} - \frac{mg}{2(R-r)} \cdot x = mx_0\omega^2 \sin(\omega t) \tag{3.8}$$

$$k = \frac{mg}{2(R-r)} = \frac{W}{l} \qquad l = \frac{x}{\varphi} \tag{3.9}$$

Due to the linearity, x(t) must be sinusoidal too. Let's assume it in the form of

$$x(t) = d \cdot \sin(\omega t) \qquad d = x_{\max} \tag{3.10}$$

Then the velocity and acceleration will be as follows

$$\dot{x}(t) = d \cdot \omega \cdot \cos(\omega t) \tag{3.11}$$

$$\ddot{x}(t) = -d \cdot \omega^2 \cdot \sin(\omega t) \tag{3.12}$$

Putting all the terms together, the equation of motion can be written as

$$-md\omega^2 \sin(\omega t) + \frac{mg}{l} d \sin(\omega t) = mx_0 \omega^2 \sin(\omega t) \tag{3.13}$$

Let's substitute

$$x_0 \omega^2 = Ag \tag{3.14}$$

Then

$$-md\omega^2 \sin(\omega t) + \frac{mg}{d} \varphi_{\max} d \sin(\omega t) = mAg \sin(\omega t) \tag{3.15}$$

If we solve the above equation for d we obtain

$$d = (A - \varphi) g / \omega^2 = D_C \tag{3.16}$$

3.3.2. Path A Response

The second path type is formed by conical plates without rounding cone apex. Let us derive response to bang-bang control of this system. The equation of motion will be in the form of

$$\ddot{x} + \varphi \cdot g \cdot \operatorname{sgn}(x) = x_0 \cdot \omega^2 \cdot \operatorname{sgn}(\sin(\omega t)) \tag{3.17}$$

Where x is equal to

$$x_1 = -at(t - \pi / \omega) \quad \text{when} \quad 0 < t < \pi / \omega$$

$$x_2 = -a(t - \pi/\omega)(t - 2\pi/\omega) \quad \text{when} \quad \frac{\pi}{\omega} < t < \frac{2\pi}{\omega} \tag{3.18}$$

Where a is unknown. If we differentiate once and twice about t velocities and accelerations

$$\dot{x}_1 = -a(2t - \pi/\omega) \quad \text{when} \quad 0 < t < \frac{\pi}{\omega}$$

$$\dot{x}_2 = -a(2t - \frac{3\pi}{\omega}) \quad \text{when} \quad \frac{\pi}{\omega} < t < \frac{2\pi}{\omega} \tag{3.19}$$

and

$$\ddot{x}_1 = -2a \quad \text{when} \quad 0 < t < \frac{\pi}{\omega}$$

$$\ddot{x}_2 = 2a \quad \text{when} \quad \frac{\pi}{\omega} < t < \frac{2\pi}{\omega} \tag{3.20}$$

Substituting these values into the equation of motion we obtain

$$-2a - \varphi g \pm x_0\omega^2 = 0$$

$$2a - \varphi g \pm x_0\omega^2 = 0 \tag{3.21}$$

then

$$a = 1/2(\varphi g \pm x_0\omega^2) \tag{3.22}$$

The maximum displacement will occur at $\frac{\pi}{2\omega}$ so that

$$d = \frac{1}{2} \cdot (\varphi g \pm x_0\omega^2) \cdot (\frac{\pi}{2\omega}) \cdot (\frac{\pi}{2\omega} - \frac{\pi}{\omega}) \tag{3.23}$$

$$d = (-\varphi g + x_0\omega^2)(\frac{\pi^2}{8\omega^2}) \tag{3.24}$$

Let us write

$$Ag = x_0\omega^2 \tag{3.25}$$

.*d* can be further simplified using the above substitution as

$$d = (\frac{\pi^2}{8})(A-\varphi)g/\omega^2 = (\frac{\pi^2}{8})D_C = D_A \tag{3.26}$$

If we consider a less severe base excitation in sinusoidal form, the equation of motion will be

$$\ddot{x} + \varphi \cdot g \cdot \mathrm{sgn}(x) = x_0\omega^2 \sin(\omega t) \tag{3.27}$$

By integrating the above equation once over t the velocities will be obtained as follows

$$\begin{aligned} \dot{x}\ (t) &= \dot{x}(0) + \varphi g t + x_0\omega(\cos(\omega t) - 1) && 0 < t < \frac{\pi}{\omega} \\ \dot{x}_2(t) &= \dot{x}(0) - \varphi g(2\pi/\omega - t) + x_0\omega(\cos(\omega t) - 1) && \frac{\pi}{\omega} < t < \frac{2\pi}{\omega} \end{aligned} \tag{3.28}$$

Since initially x(0)=0 (steady state motion), by further integration the displacements will be obtained as

$$\begin{aligned} x_1(t) &= (\dot{x}(0) - x_0\omega)t + x_0 \sin\omega t + \varphi g t^2/2 && 0 < t < \frac{\pi}{\omega} \\ x_2(t) &= (\dot{x}(0) - x_0\omega)t + x_0 \sin\omega t - \varphi g\left[\frac{t^2}{2} - \frac{2\pi}{\omega}t - \frac{\pi^2}{\omega^2}\right] && \frac{\pi}{\omega} < t < \frac{2\pi}{\omega} \end{aligned} \tag{3.29}$$

At the half period $\left(t = \frac{\pi}{\omega}\right)$ the displacement is zero which yields to

$$x\left(\pi/\omega\right) = 0 = \dot{x}(0)\frac{\pi}{\omega} - x_0\omega\frac{\pi}{\omega} + 0 + \varphi g\left(\frac{\pi}{\omega}\right)^2 / 2$$

$$\dot{x}(0) = x_0\omega - \varphi g\pi / 2\omega \tag{3.30}$$

The maximum displacement will be

$$x(t) = -\varphi g\frac{\pi}{2\omega}t + x_0 \sin\omega t + \varphi g\frac{t^2}{2} \tag{3.31}$$

$$x\left(\frac{\pi}{2\omega}\right) = 0$$

$$x_{\max} = x\left(\frac{\pi}{\omega}\right) = -\varphi g\frac{\pi^2}{4\omega^2} + x_0 + \varphi g\frac{\pi^2}{8\omega^2} = x_0 - \varphi g\frac{\pi^2}{8\omega^2} \tag{3.32}$$

Which simply yields to

$$A = x_0\frac{\omega^2}{g} \qquad\qquad d = \left[A - \varphi\left(\frac{\pi^2}{8}\right)\right]\cdot\frac{g}{\omega^2} = D'_A \tag{3.33}$$

Which is smaller than D_A and D_C.

3.3.3. Path B Response

The third type is a system with conical plates and rounded cone apex. Here we must introduce a sign function (signum function) without jump instead of heavy side step function, to deal with the derivation of the response of the system to bang-bang control without jumps (rounding involves smooth linear passage of the ball from apex region).

The cone apex radius being equal to $\varepsilon d / 2\varphi$, we will have six pieces of responses in a period with discontinuities at 0, ε, $\left(\frac{\pi}{\omega-\varepsilon}\right)$, $\left(\frac{\pi}{\omega+\varepsilon}\right)$, $\left(\frac{2\pi}{\omega-\varepsilon}\right)$, $\left(\frac{2\pi}{\omega}\right)$.

The equation of motion will be as follows

$$\ddot{x} + \varphi g \operatorname{sgn}^*(x) = x_0 \omega^2 \sin(\omega t) \tag{3.34}$$

Here the sgn^* function represents sign function (signum function) without jump. Integrating the above equation the velocities will be obtained as

$$\begin{aligned}
\dot{x}_1(t) &= \dot{x}(0) + x_0\omega(\cos(\omega t) - 1) + \varphi g\left(\frac{t^2}{2\varepsilon}\right) && 0 < t < \varepsilon \\
\dot{x}_2(t) &= \dot{x}(0) + x_0\omega(\cos(\omega t) - 1) + \varphi g(t - \varepsilon/2) && \varepsilon < t < \pi/\omega - \varepsilon \\
\dot{x}_3(t) &= \dot{x}(0) + x_0\omega(\cos(\omega t) - 1) + \varphi g\left(-\frac{(t-\pi/\omega)^2}{2\varepsilon} - \frac{\varepsilon}{2} + \frac{\pi}{\omega}\right) && \pi/\omega - \varepsilon < t < \pi/\omega
\end{aligned} \tag{3.35}$$

In steady state motion x(0) being equal to zero, by further integration the displacements will be obtained as

$$x(t) = (\dot{x}(0) - x_0\omega)t + x_0 \sin\omega t + \varphi g \begin{Bmatrix}
\frac{t^3}{6\varepsilon} & 0 < t < \varepsilon \\
\frac{t^2}{2} - \frac{\varepsilon t}{2} + \frac{\varepsilon^2}{6} & \varepsilon < t < \frac{\pi}{\omega} - \varepsilon \\
-\frac{(t-\pi/\omega)^3}{6\varepsilon} + \left(\frac{\pi}{\omega} - \varepsilon\right)\left(t - \frac{\pi}{2\omega}\right) & \frac{\pi}{\omega} - \varepsilon < t < \frac{\pi}{\omega} + \varepsilon \\
-\frac{t^2}{2} + \frac{2\pi}{\omega}t - \frac{\varepsilon}{2}t - \frac{\pi^2}{\omega^2} - \frac{\varepsilon^2}{6} & \frac{\pi}{\omega} + \varepsilon < t < \frac{2\pi}{\omega} - \varepsilon \\
\frac{(t-2\pi/\omega)^3}{6\varepsilon} + \frac{\pi^2}{\omega^2} - \frac{\pi}{\omega}\varepsilon & \frac{2\pi}{\omega} - \varepsilon < t < \frac{2\pi}{\omega}
\end{Bmatrix} \tag{3.36}$$

At $t = \frac{\pi}{\omega}$ the displacement is zero which yields to

$$x\left(\frac{\pi}{\omega}\right) = 0 = x(0)\frac{\pi}{\omega} - x_0\omega\frac{\pi}{\omega} + 0 + \varphi g\left(\frac{\pi}{\omega} - \varepsilon\right)\frac{\pi}{2\omega} \tag{3.37}$$

$$\dot{x}(0) = x_0\omega - \varphi g\left(\frac{\pi}{\omega} - \varepsilon\right)\frac{1}{2}$$

The above equations for the displacements can now be written in the form of

$$x(t) = -\varphi g\left(\frac{\pi}{\omega} - \varepsilon\right)t + x_0 \sin\omega t + \varphi g.\{...\} \tag{3.38}$$

The maximum displacement can be calculated by solving the equation at $t = \frac{\pi}{2\omega}$

$$x\left(\frac{\pi}{2\omega}\right) = d = -\frac{\varphi g\pi^2}{8\omega^2} + \frac{\varphi g\varepsilon^2}{6} + x_0 \tag{3.39}$$

$$Ag = x_0\omega^2 \qquad d = \frac{g}{\omega^2}\left(A - \varphi\left(\frac{\pi^2}{8} + \frac{\omega^2\varepsilon^2}{6}\right)\right) = D_B \tag{3.40}$$

Which is smaller than D_c and D_A derived before.

3.4. Simple Method of Analysis (due to Uniform Building Code (UBC) 1997)

D is design displacement of isolation system, D_T is total displacement of isolation system, T_I is the isolation period, Z is the seismic zone factor.

$$B \approx \left(\frac{8}{\pi}\right)\beta^{1/3} \tag{3.40}$$

where β is damping of the isolation system. F is the restoring force proportional to displacement anf Q is the dissipative force proportional to velocity.

$$\varphi = \frac{F}{w} \quad (\text{constant}) \tag{3.41}$$

$$\alpha = \frac{Q}{w} \quad (\text{constant}) \tag{3.42}$$

$$C = \frac{F+Q}{w} \quad (\text{constant}) \tag{3.43}$$

Spectral displacement from damped spectrum at $T = T_I$ is:

$$D = \frac{10 \cdot Z \cdot S_I \cdot T_I}{B} \tag{3.44}$$

$$T_I = 2\pi\sqrt{\frac{W}{k_{\min} g}} \tag{3.45}$$

Where;

$$k_{\min} = k_{\max} = k = \frac{C \cdot W}{D} = \frac{C \cdot W \cdot 4\pi^2}{g \cdot C \cdot T_I^2} = m\omega_I^2 \tag{3.46}$$

and where,

$$m = \frac{w}{g} \tag{3.47}$$

$$\omega_I = \frac{2\pi}{T_I} \tag{3.48}$$

So;

$$D = \frac{g \cdot C \cdot T_I^2}{4\pi^2} \tag{3.49}$$

$$T_I = \frac{Z \cdot N_I \cdot S_I}{B \cdot C} \tag{3.50}$$

$$\beta = \frac{2\alpha}{\pi\left(\alpha + \varphi\right)} = \frac{2\alpha}{\pi C} \tag{3.51}$$

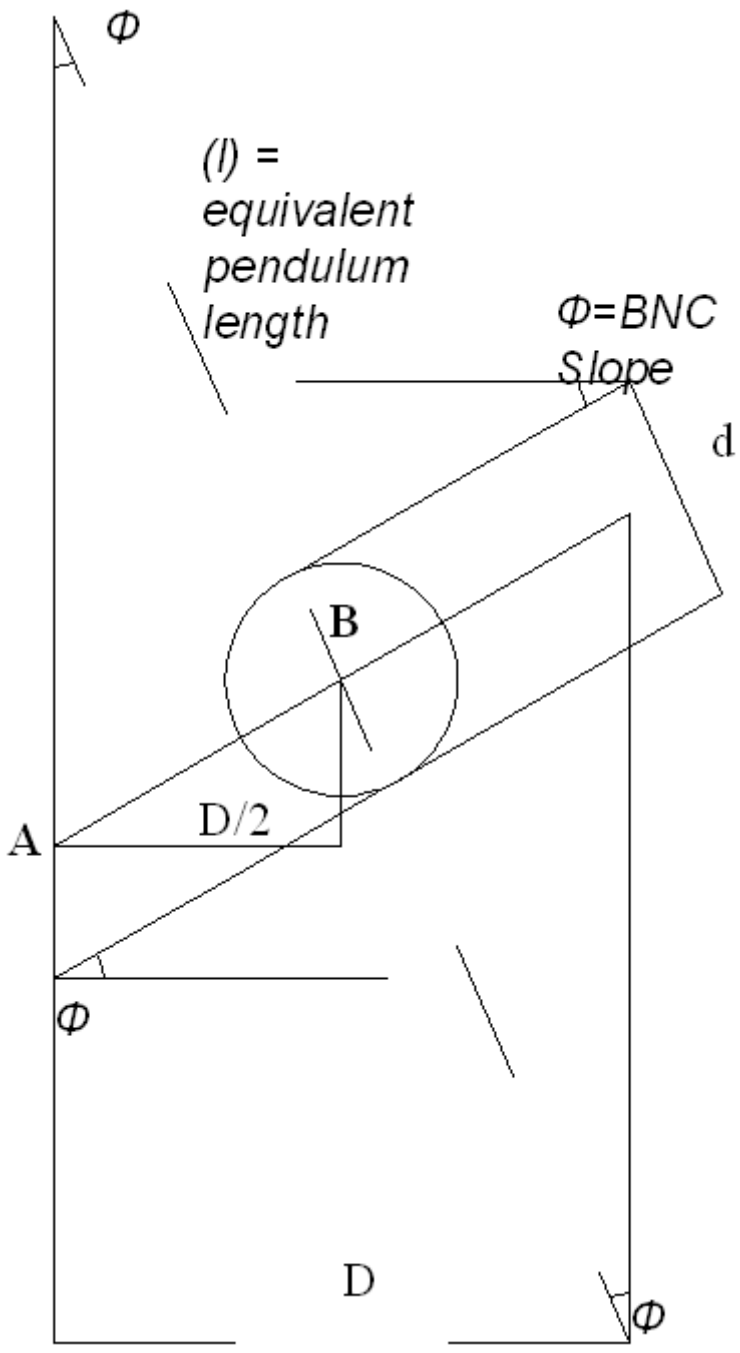

Figure 3.4 Cone geometry for seismic displacement

D is the seismic displacement and d is the ball diameter.

$$AC = \frac{D}{2} = AB \cdot \cos\phi \tag{3.52}$$

$$AB = \frac{D}{2} \cdot \frac{1}{\cos\phi} \tag{3.53}$$

$$AB \Big/ \frac{L}{2} = \tan\phi \tag{3.54}$$

$$\frac{L}{2} = \frac{AB}{\tan\phi} \tag{3.55}$$

If we substitute,

$$\frac{L}{2} = \frac{\frac{D}{2}}{\cos\phi \cdot \tan\phi} \tag{3.56}$$

$$L = \frac{D}{\cos\phi \cdot \tan\phi} \tag{3.57}$$

l is the equivalent length;

$$l = L - d \tag{3.58}$$

For small ϕ in radian

$$l \approx \frac{D-d}{\phi} \tag{3.59}$$

$$D = \frac{10Z \cdot N \cdot S_I \cdot T_I}{B} \tag{3.60}$$

Where, *D* is seismic displacement, *Z* is seismic zone base shear, *N* is the site soil profile, S_I is the isolation period, T_I is the damping coefficient and "10" comes from π^2.

$$D\ \left(\text{Spectral displacement}\right) = \frac{SA}{\omega^2} \tag{3.61}$$

Where,

$$\omega^2 = \left(2\pi f\right)^2 = \frac{4\pi^2}{T^2} \tag{3.62}$$

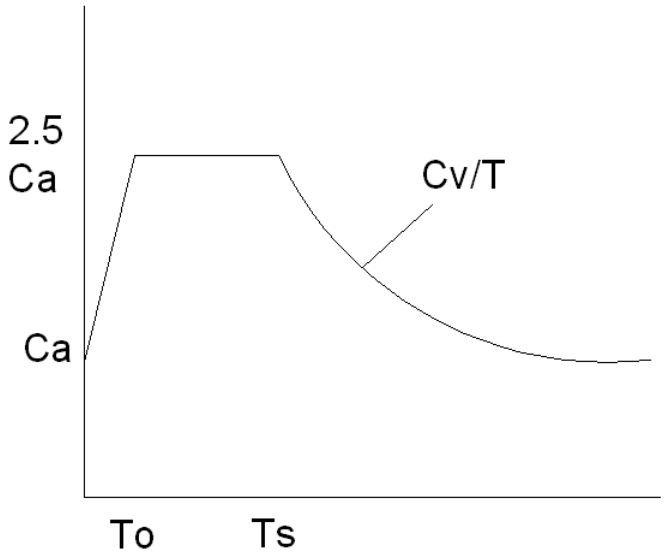

Figure 3.5 Spectral Response

$$V = \frac{C_V \cdot I}{R \cdot T} W \tag{3.63}$$

where C_V is spectral acceleration at 1 second in $inches/\sec^2$.

$$T_0 = \frac{V_C}{2.5 C_A} \tag{3.64}$$

and

$$T_S = 0.2 T_0 \tag{3.65}$$

If we substitute,

$$D = \frac{SA \cdot T^2}{4\pi^2} = \frac{\frac{C_V}{T} \cdot T^2}{4\pi^2} = \frac{C_V \cdot T}{4\pi^2} \tag{3.66}$$

If we substitute $1g = 9.81 m/s^2 = 32.18 \frac{ft}{s^2} = 386 in/\sec^2$, then,

$$D = 9.79 C_V T \tag{3.67}$$

So,

$$C_V = \frac{Z \cdot S_I}{B} \tag{3.68}$$

Where B is damping factor.

$$T_I = 2\pi \sqrt{\frac{W}{k_{\min} g}} = 2\pi \sqrt{\frac{W/g}{k_{\min}}} \tag{3.69}$$

$$f = \frac{1}{2\pi} \sqrt{\frac{g}{R-d}} = \frac{1}{2\pi} \sqrt{\frac{g}{l}} \tag{3.70}$$

So,

$$T = 2\pi \sqrt{\frac{l}{g}} = 2\pi \sqrt{\frac{W/g}{k_{\min}}} \tag{3.71}$$

$$\frac{l}{g} = \frac{W}{g \cdot k_{\min}} \tag{3.72}$$

$$k_{\min} = \frac{W}{l} = \frac{W \cdot \phi}{D-d} \tag{3.73}$$

$$T_I = 2\pi \sqrt{\frac{W/g}{W \cdot \phi / D-d}} = 2\pi \sqrt{\frac{(D-d)/\phi}{g}} = 2\pi \sqrt{\frac{l}{g}} \tag{3.74}$$

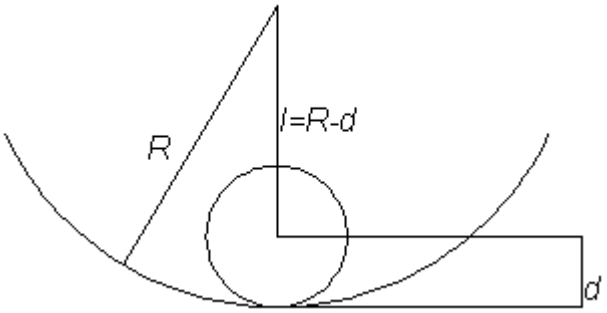

Figure 3.6 Cone geometry

So,

$$D = 10 \cdot C_V \cdot T = 10 \cdot C_V \cdot 2\pi \sqrt{\frac{D-d}{\phi g}} \tag{3.75}$$

$$D^2 = 100 \cdot C_V^2 \cdot 4\pi^2 \frac{D-d}{\phi g} = 100 \cdot C_V^2 \cdot 4 \cdot (3.14)^2 \frac{1}{386} \cdot \frac{D-d}{\phi} \tag{3.76}$$

$$D^2 = 10 \cdot C_V^2 \cdot \frac{D-d}{\phi} = \frac{10 \cdot C_V^2}{\phi} D - \frac{10 \cdot C_V^2}{\phi} d \Leftrightarrow \frac{10 \cdot C_V^2}{\phi} = \gamma \tag{3.77}$$

$$D^2 = \gamma D - \gamma d \tag{3.78}$$

$$D^2 - \gamma D + \gamma d = 0 \tag{3.79}$$

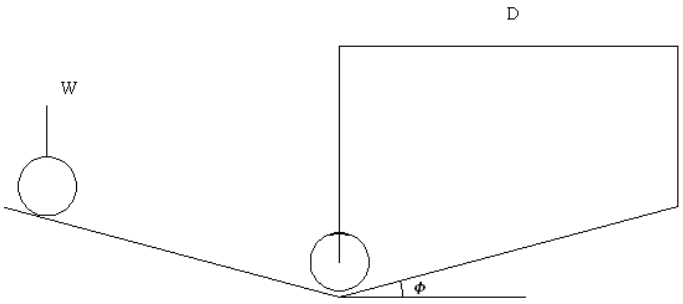

Figure 3.7 Cone slope and displacement

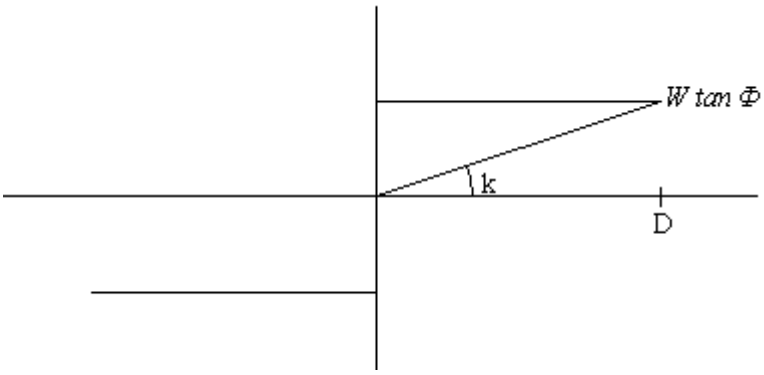

Figure 3.8 Force – displacement relationship

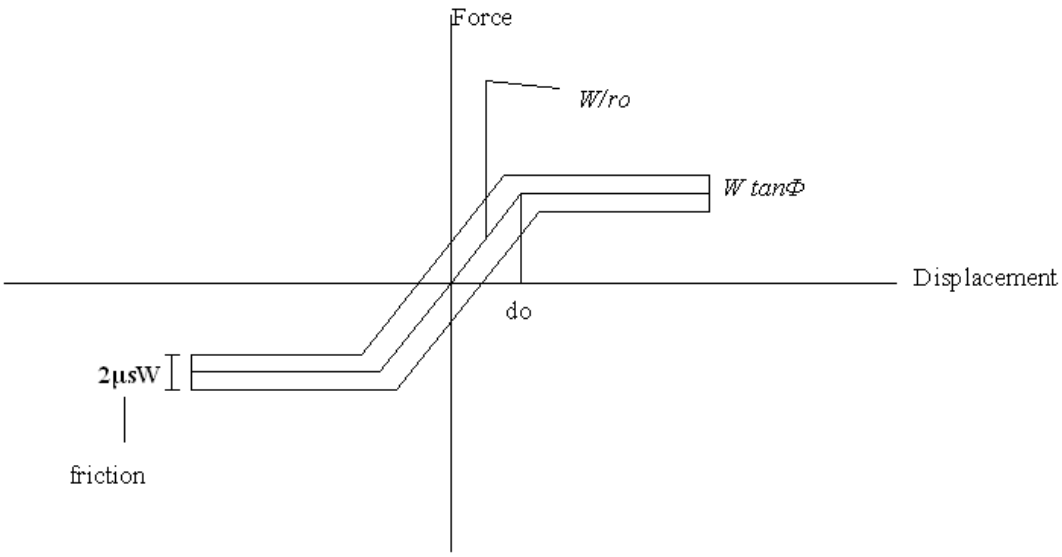

Figure 3.9 Force-displacement relationship

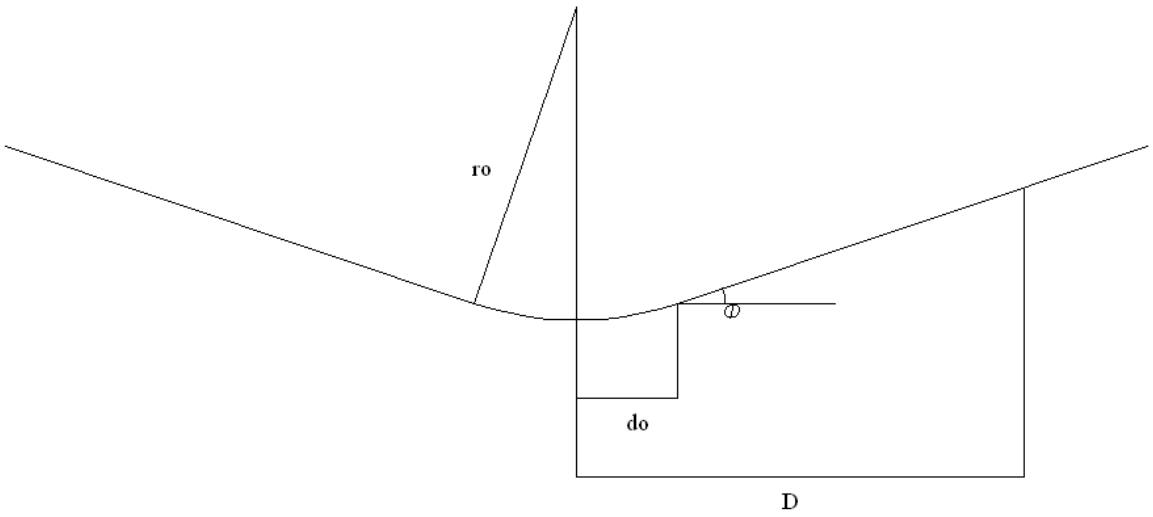

Figure 3.10 Cone geometry

$$k = \frac{W \cdot \tan\phi}{D} \approx \frac{W\phi}{D} \tag{3.80}$$

Where D is radius of the ball.

$$T_I = 2\pi\sqrt{\frac{D-d}{g\phi}} \tag{3.81}$$

$$D = SA(1s)\frac{T_I}{4\pi^2} \tag{3.82}$$

If we assume $SA = \frac{SA(1)}{T}$.

$$T_I = \frac{4\pi^2 D}{SA(1)} \tag{3.83}$$

$$2\pi\sqrt{\frac{D-d}{g\phi}} = 4\pi^2\frac{D}{SA(1)} \tag{3.84}$$

$$4\pi^2 \frac{D-d}{g\phi} = 16\pi^2 \frac{D^2}{SA^2(1)} \tag{3.85}$$

$$D - d = 4\pi^2 g\phi \frac{D^2}{SA^2(1)} = \frac{4\pi^2 g\phi}{SA^2(1)} D^2 \tag{3.86}$$

If $a\chi^2 + b\chi + c = 0 \Rightarrow \chi = -\frac{b}{2a} \pm \frac{\sqrt{b^2 - 4ac}}{2a}$.

$$\frac{4\pi^2 g\phi}{SA^2(1)} D^2 - D + d = 0 \tag{3.87}$$

$$D = +\frac{1}{2\left(\frac{4\pi^2 g\phi}{SA^2(1)}\right)} \pm \frac{\sqrt{1 - 4\left(\frac{4\pi^2 g\phi}{SA^2(1)}\right)}}{2\left(\frac{4\pi^2 g\phi}{SA^2(1)}\right)} \tag{3.88}$$

$$D = +\frac{1}{8\pi^2 g\phi} SA^2(1) \pm \frac{\sqrt{1 - \left(16\pi^2 g\phi \cdot \frac{1}{SA^2(1)}\right)}}{\left(\frac{8\pi^2 g\phi}{SA^2(1)}\right)} \tag{3.89}$$

$$D = +\frac{1}{8\pi^2 g\phi}\left[SA^2(1) \pm SA^2(1)\sqrt{1 - 16 g\phi \cdot \frac{1}{SA^2(1)}} \right] \tag{3.90}$$

$$D = +\frac{1}{8\pi^2 g\phi} \cdot SA^2(1)\left[1 \pm \sqrt{1 - 16 g\phi \cdot \frac{1}{SA^2(1)}} \right] \tag{3.91}$$

3.5 Model and Prototype

A true scale prototype is developed for analysis. A Ball iN Cone (BNC) with a 330 mm diameter conical plate and a ball with a radius 45mm. The conical surface gradient is decided as $\varphi = 0.08 = 8\%$. In this respect we would like to express our special thanks to Eren Kalafat and Ulus Yapı for their assistance in providing and manufacturing the BNC devices.

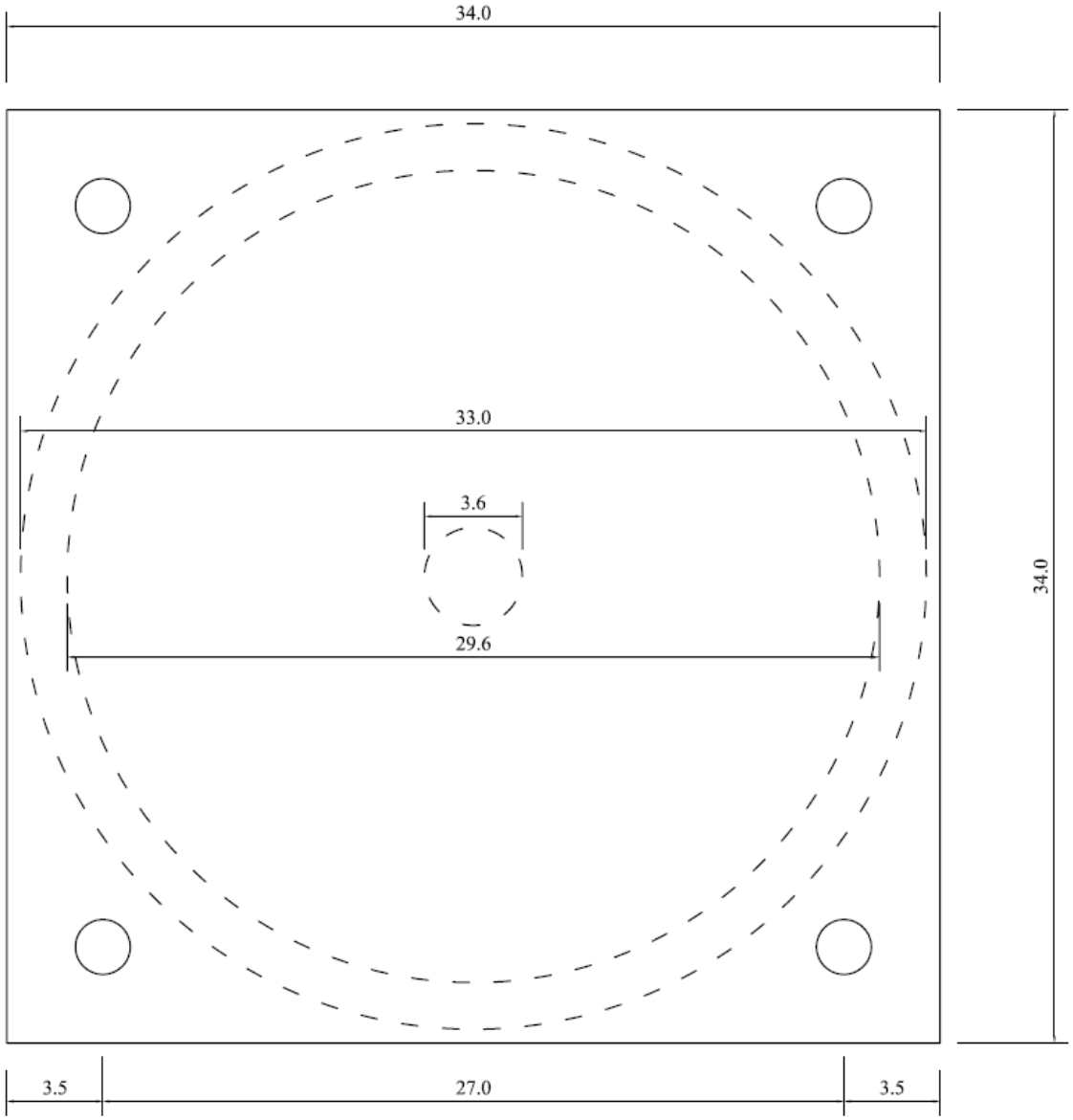

Figure 3.11.a Prototype BNC's geometry

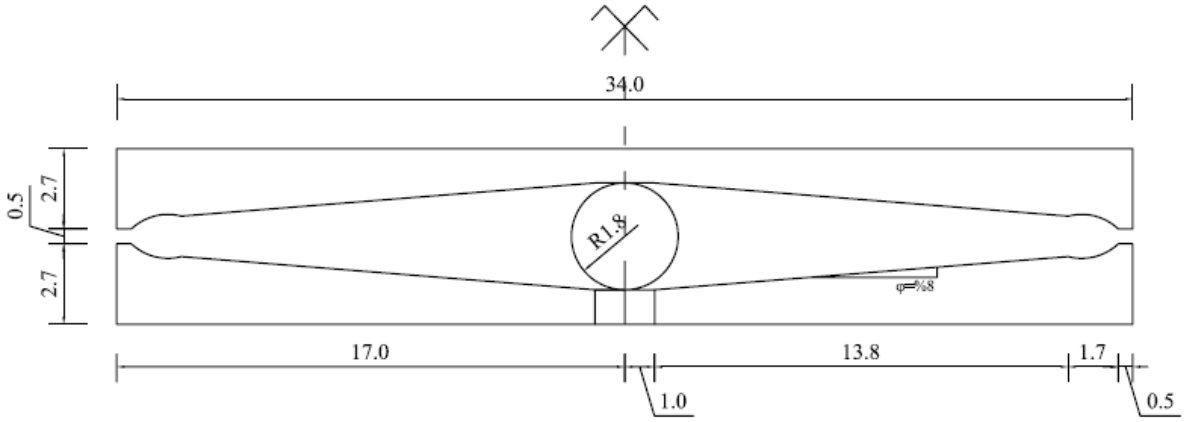

Figure 3.11.b Cross-Section of BNC

Measurements of conical plates' geometry in the laboratory have shown that the prototype made according to the model has good precision. The shaking table test records taken to understand the characteristics of BNC.

In theory the BNC system is frictionless. In contrast to this, not only all materials has friction in nature, but also low frictionless materials are relatively expensive. In addition to this, the system generated some friction forces.

3.6. The Structural System

A model natural scale steel structure is devised, and made by DO-KA Steel Formwork and Machinery Ltd., based on four slabs of steel (Figure 3.12). The structure has 1,5 ton weight. Nevertheless, we added 1,5 ton extra load on the top slab. (Figure 3.13)

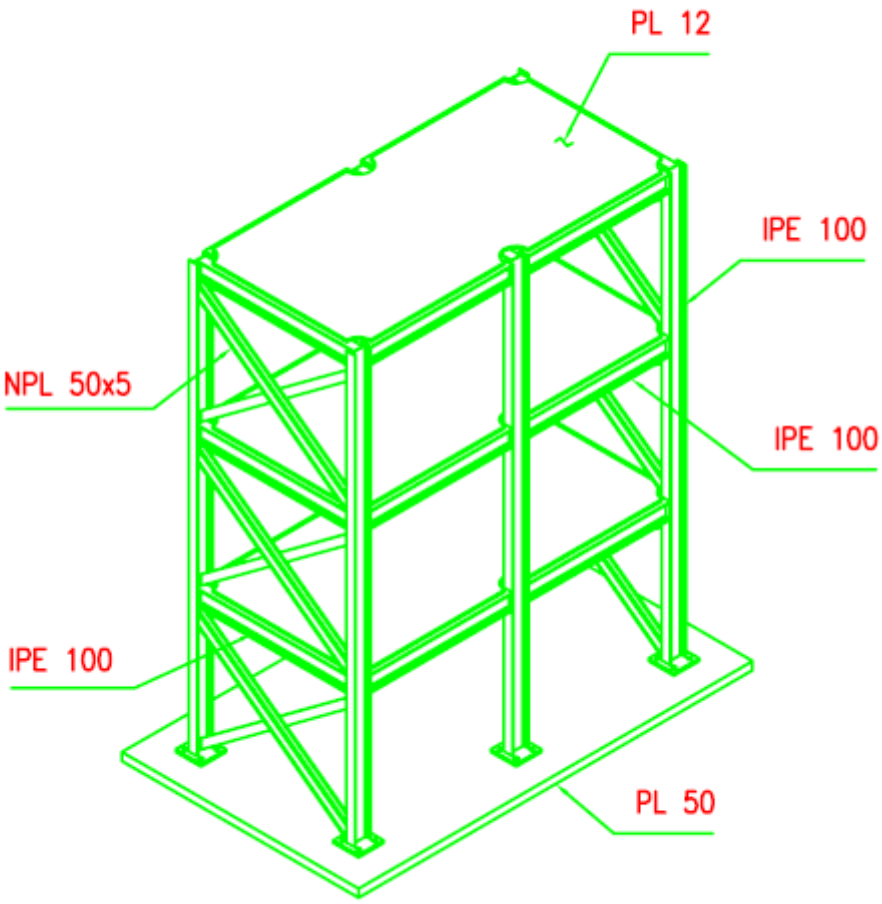

Figure 3.12 Steel structure used for the test

Figure 3.13 Additional masses (1.5 ton) added on the top of the system

3.7 Testing

Tests were done in Boğaziçi University Kandilli Observatory and Earthquake Research Institute, Earthquake Engineering Department's Shaking Table laboratory. Four BNC bearing (Figure 3.14) which were provided by Ulus Yapı is used. A natural scale steel structure is devised, and made by DO-KA, based on four slabs of steel. In addition to the system, masses which is totally 1,5 ton were added at the top storey of the system as shown in Figure 3.13. The ground motion with a frequency of 0.5 to 5 Hz is given to the system. The acceleration time history is taken by eight accelerometers. Also displacements are measured by three LVDT which are settled on the shake table, base and the top of the system. Testing scheme is shown in Figure 3.15

Figure 3.14 One of the BNC bearings that is settled under the system

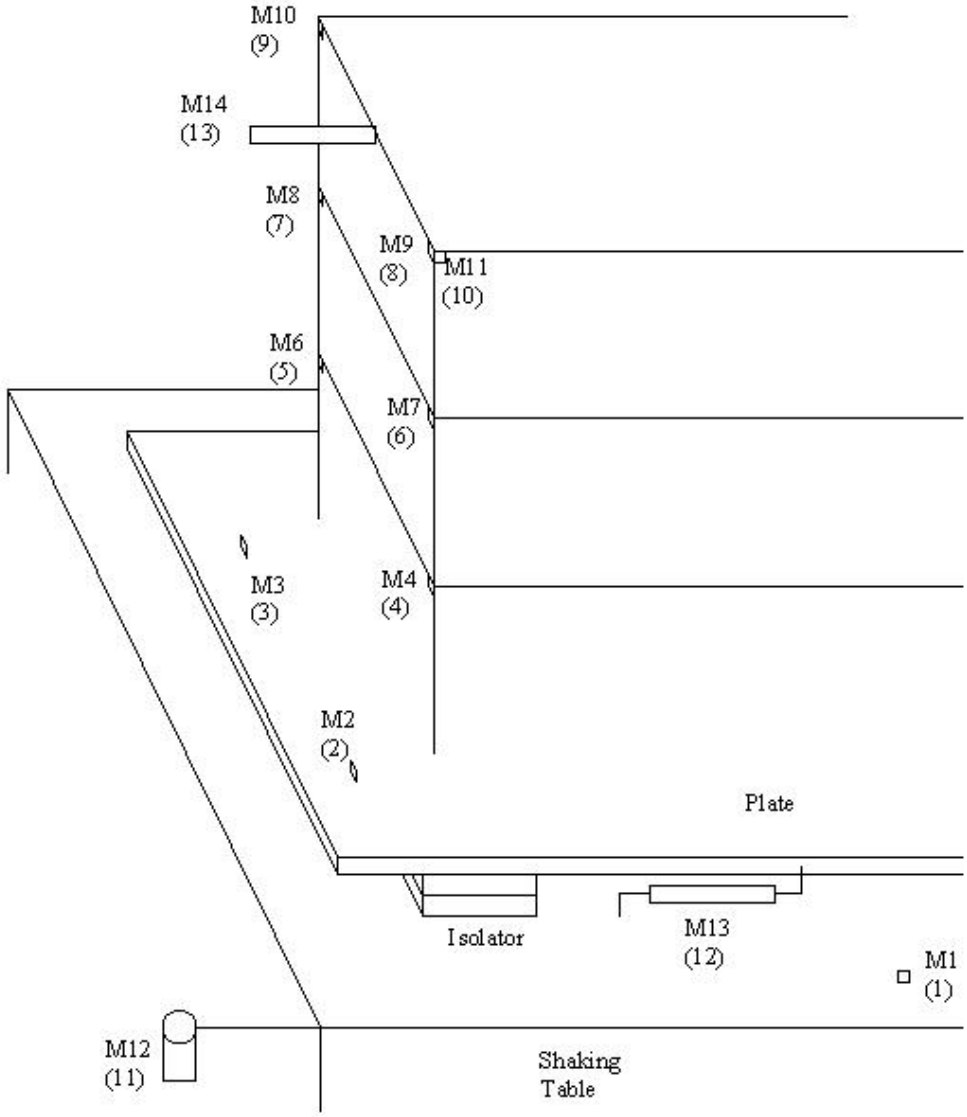

Figure 3.15 Testing Scheme

Table 3.1 Instruments and their functions

Instrument	Function
M1 (1)	Measuring Input Motion
M2 (2)	Acceleration of base
M3 (3)	Acceleration of base
M4 (4)	Acceleration 1st floor
M6 (5)	Acceleration 1st floor
M7 (6)	Acceleration 2nd floor
M8 (7)	Acceleration 2nd floor
M9 (8)	Acceleration 3rd floor
M10 (9)	Acceleration 3rd floor
M11 (10)	Acceleration out of plane (top)
M12 (11) – LVDT 1	Displacement of input motion
M13 (12) – LVDT 2	Displacement of base
M14 (13) – LVDT 3	Displacement of top

Nevertheless, due to damaged and wrong output, the instruments, M2, M3, M11, M13 (LVDT2), M14 (LVDT3) are eliminated.

3.8 Test Results

The results are taken for each frequency (0.5 Hz, 1 Hz, 2 Hz, 3 Hz, 4 Hz, 5 Hz). The outputs are taken from each instrument except the eliminated instruments. The ground motion with a frequency of 4 Hz and it's outputs are given in Figure 3.16 to 3.23. The other results are shown in Table 3.2 ~ 3.5.

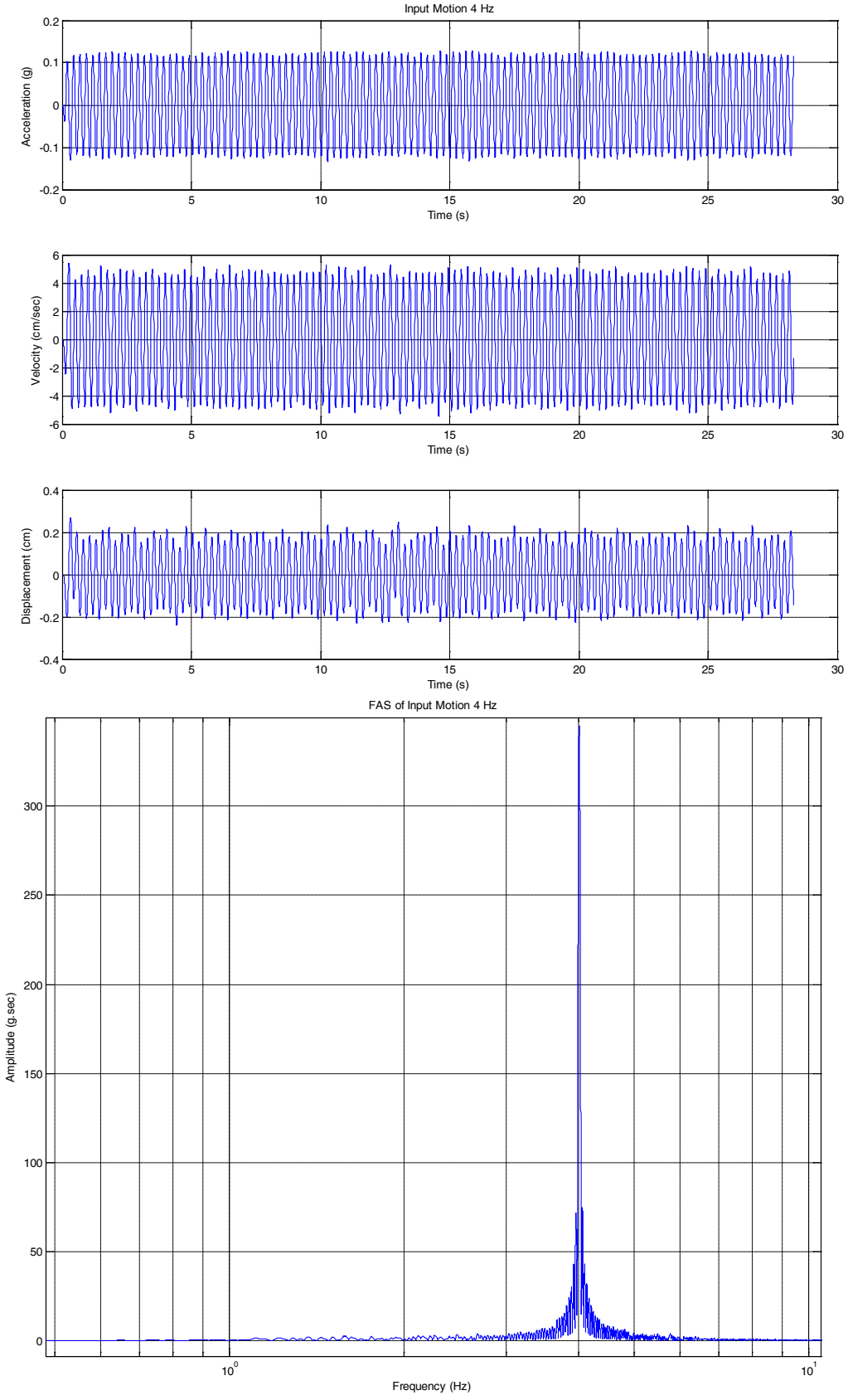

Figure 3.16 Input Motion and its FAS (4 Hz)

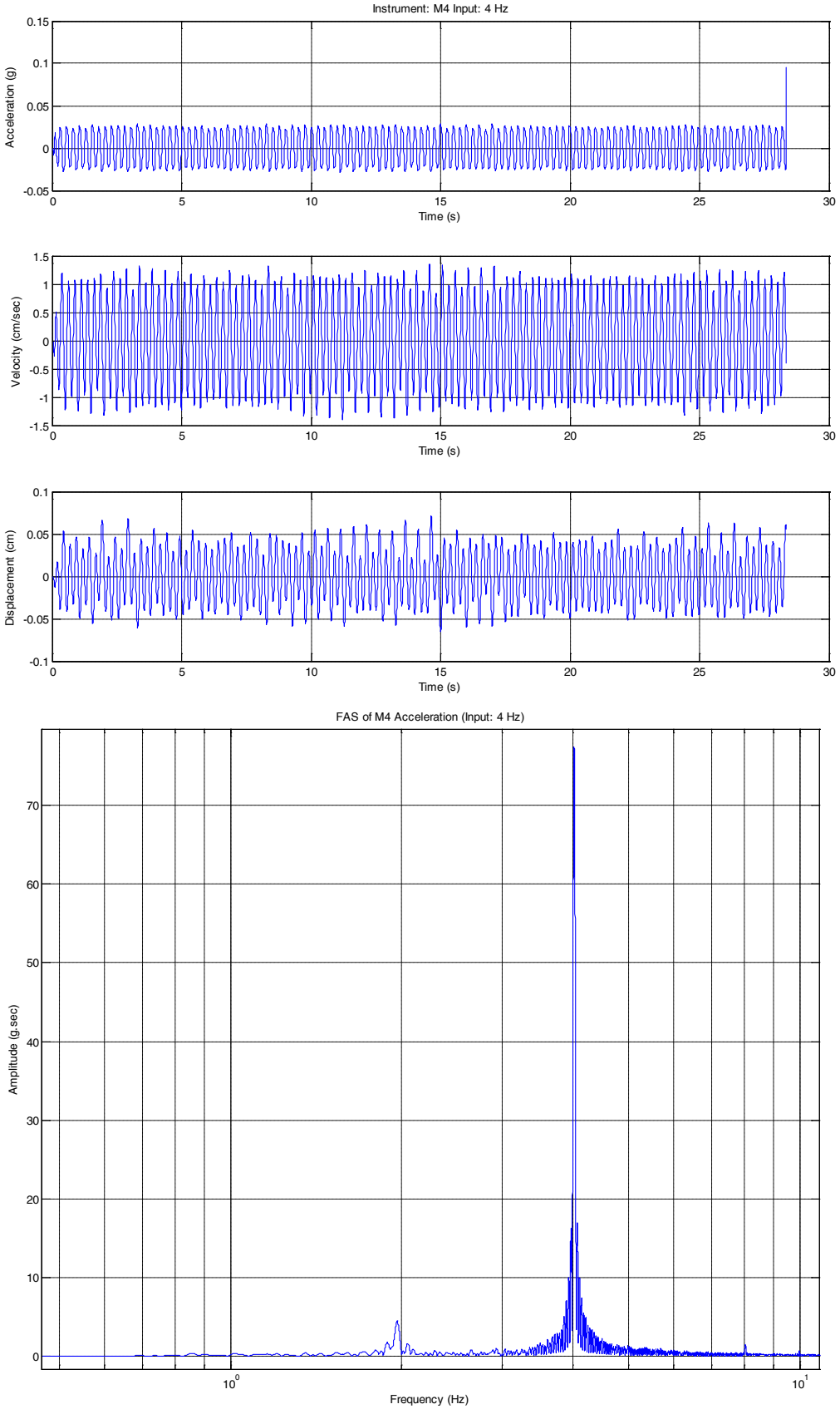

Figure 3.17 The output taken from instrument M4

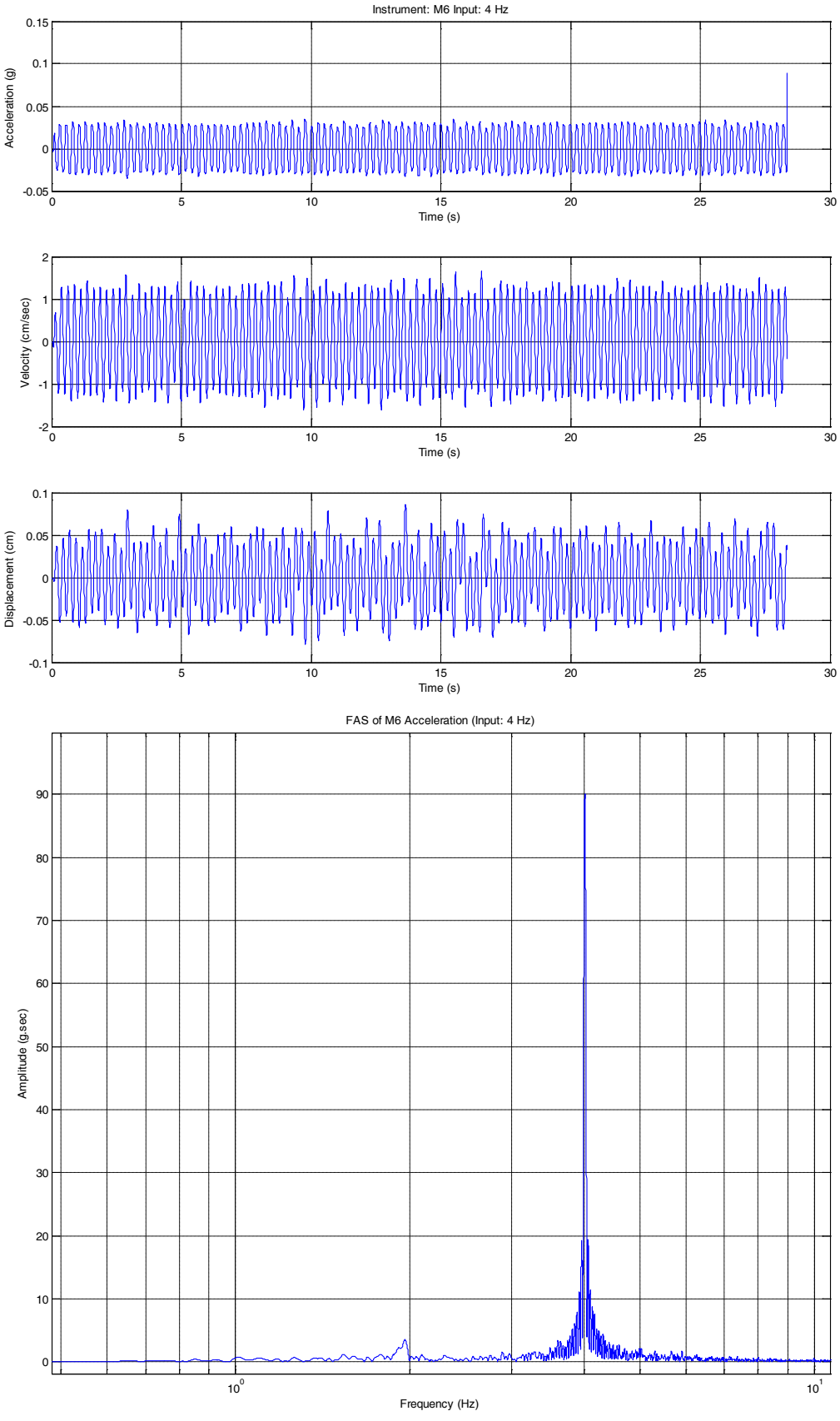

Figure 3.18 The output taken from instrument M6

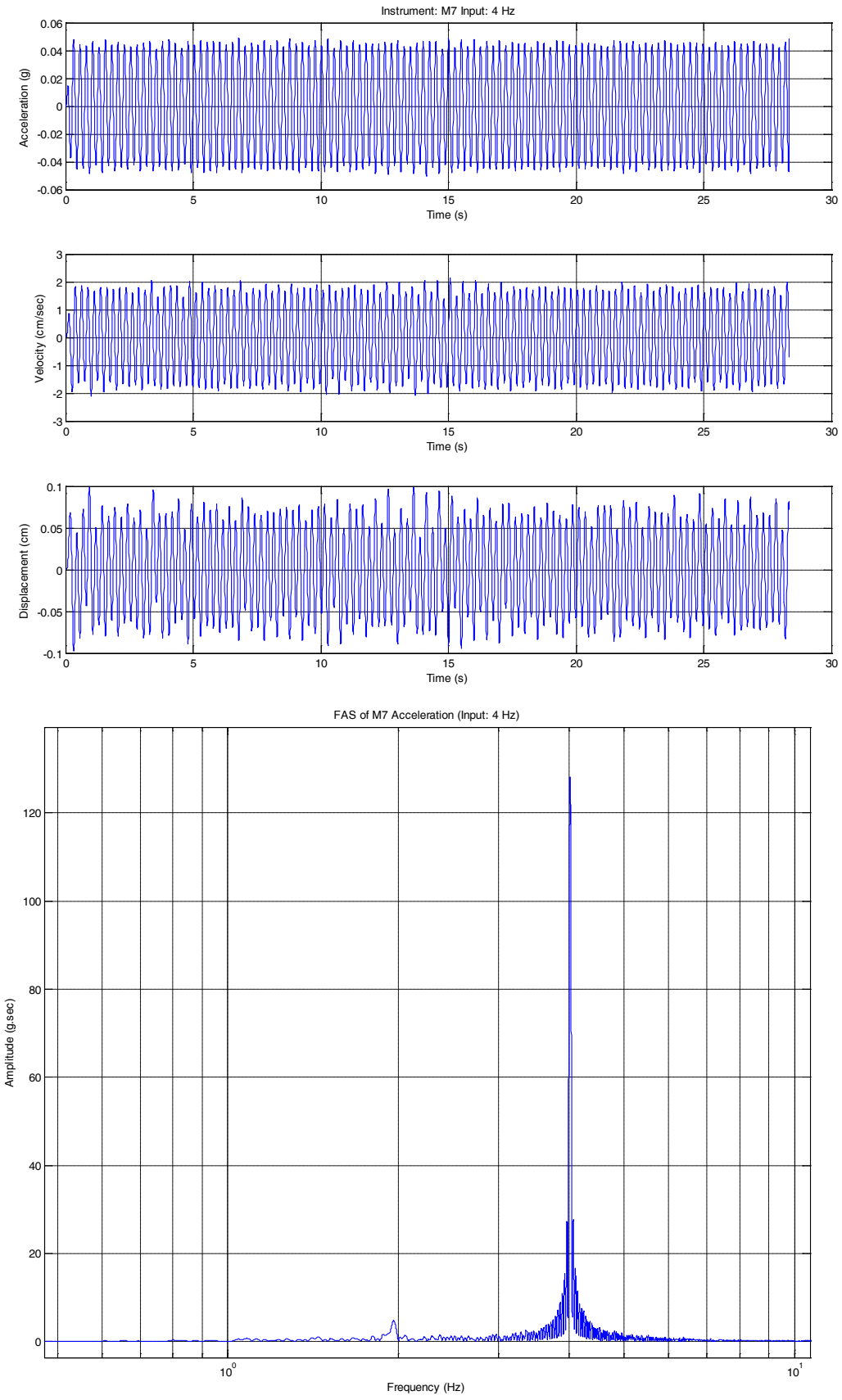

Figure 3.19 The output taken from instrument M7

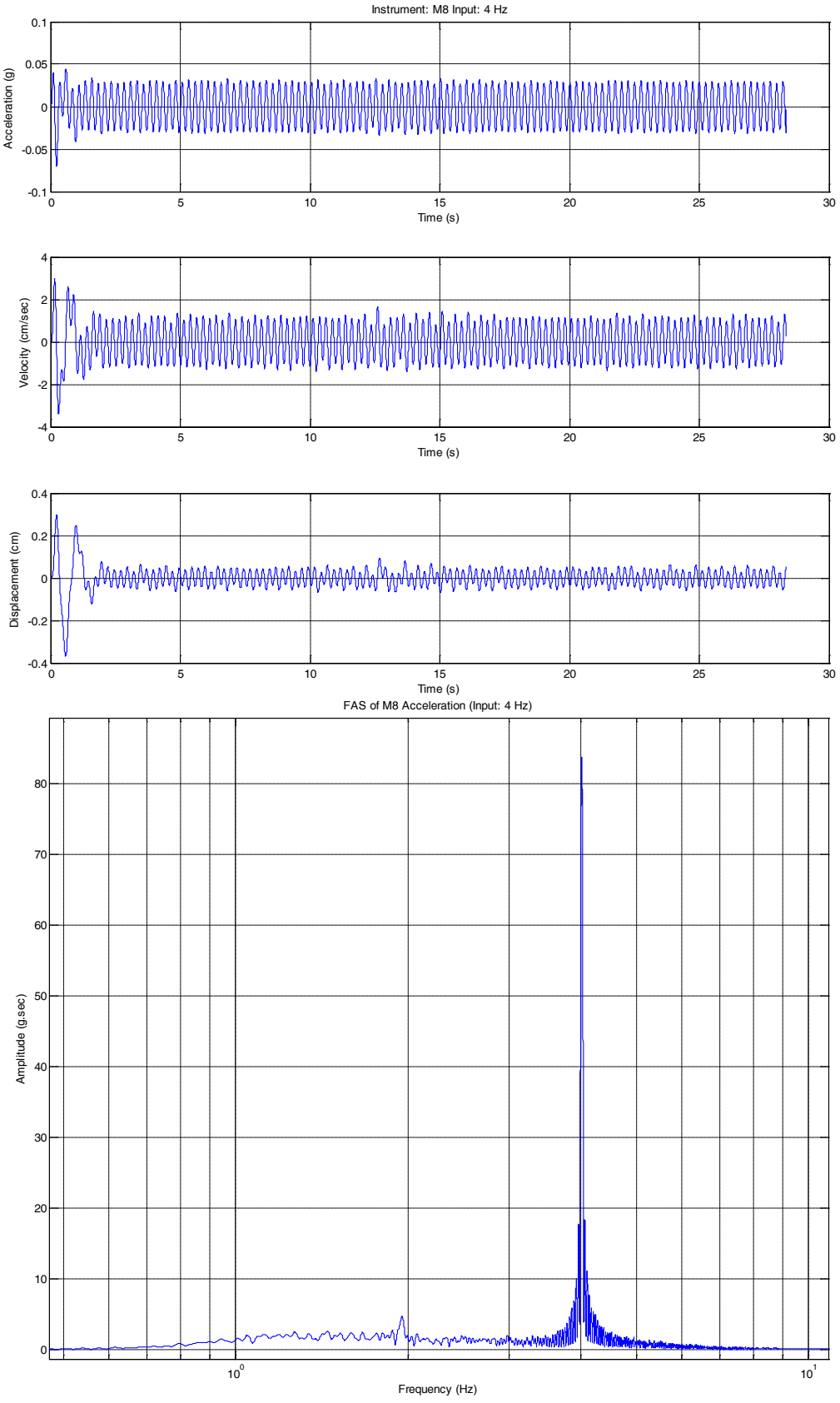

Figure 3.20 The output taken from instrument M8

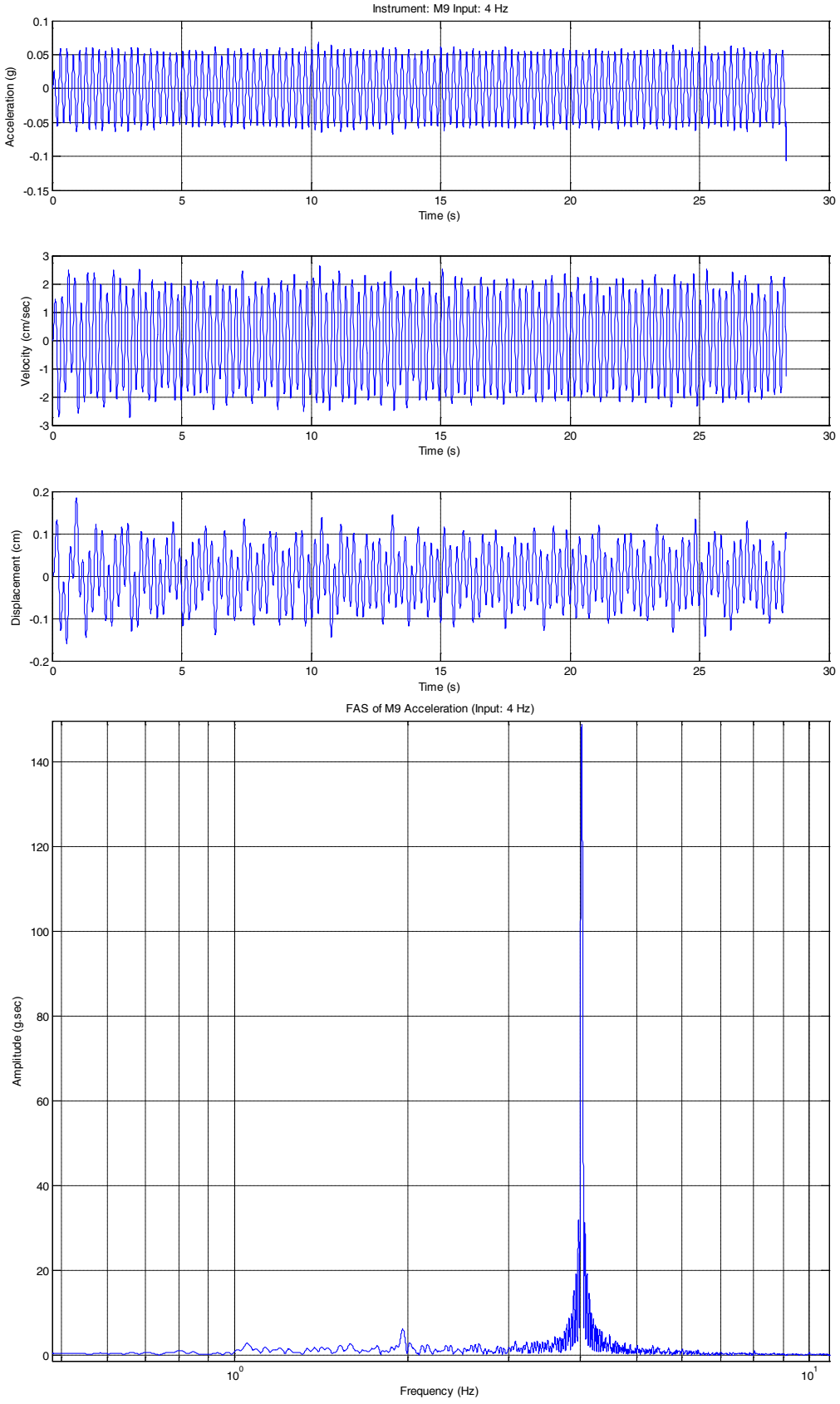

Figure 3.21 The output taken from instrument M9

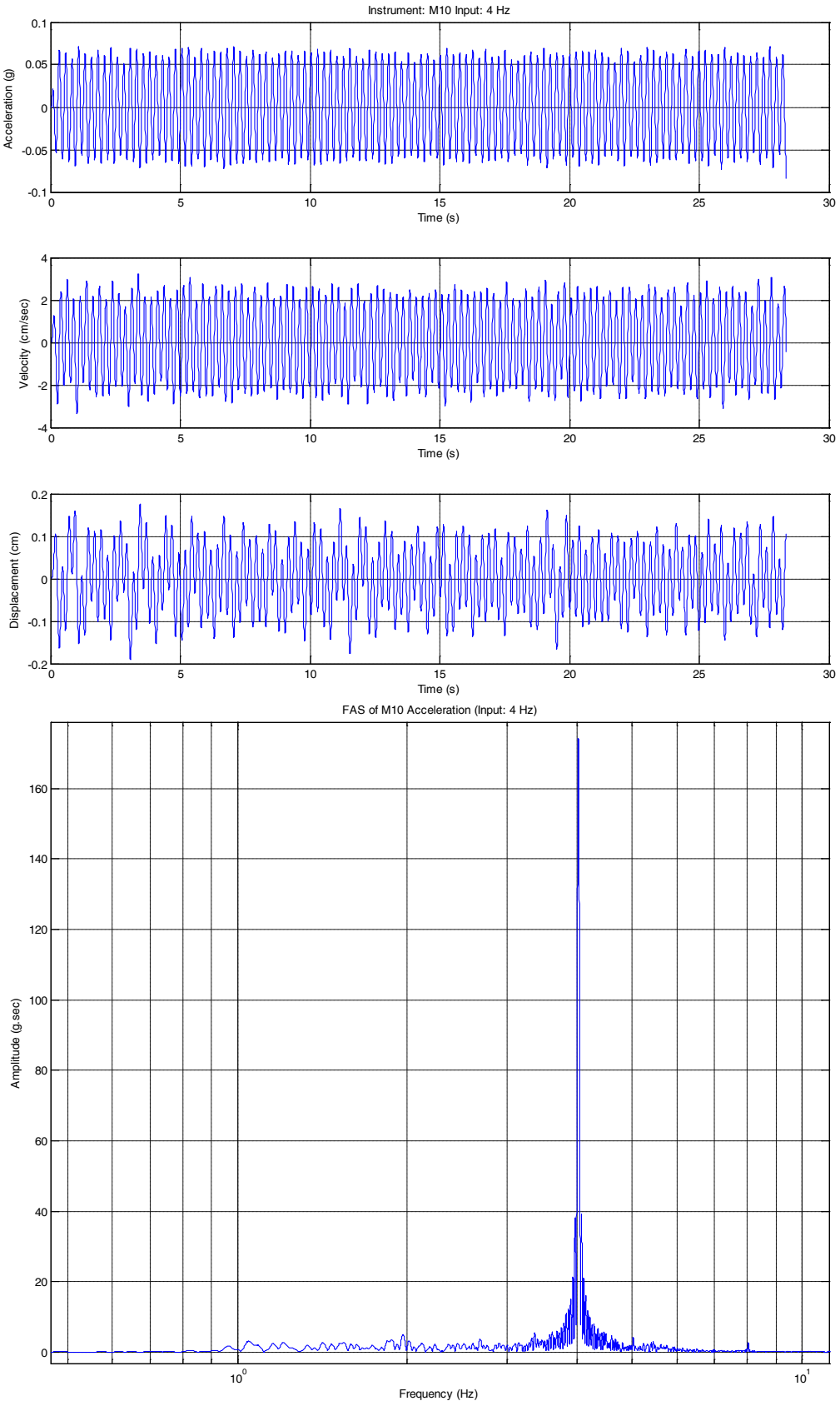

Figure 3.22 The output taken from instrument M10

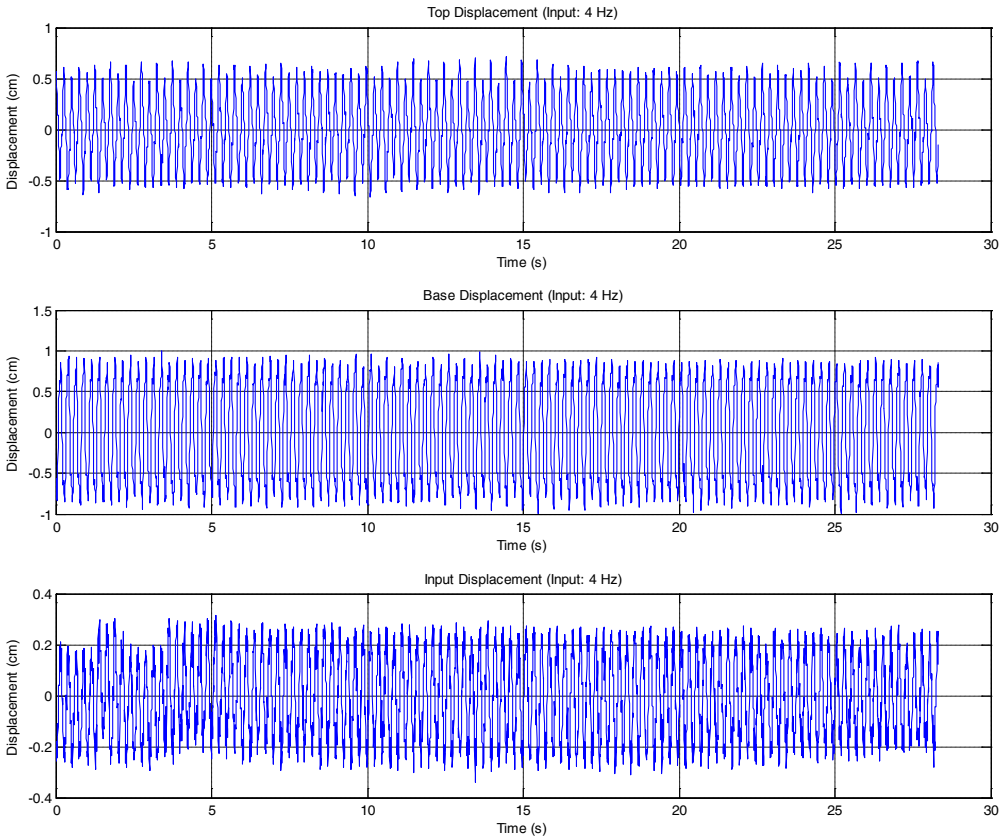

Figure 3.23 The output of displacements which is measured by the instruments M12 (LVDT1), M13 (LVDT2), M14 (LVDT3) however because of damaging M13 and M14's records are eliminated.

Table 3.2 The input motions

Frequency	INPUT			LVDT 1
	Acc (g)	Vel (cm/sec)	Disp (cm)	Displacement of Input (cm)
0.5 Hz	0.01	1	0.3	0.3
1 Hz	0.015	2	0.35	0.35
2 Hz	0.04	2.5	0.2	0.2
3 Hz	0.07	4	0.2	0.3
4 Hz	0.1	5	0.3	0.3
5 Hz	0.15	6	0.3	0.3

Table 3.3 The output which is measured in first floor

Frequency	(M4+M6)/2		
	Acc (g)	Vel (cm/sec)	Disp (cm)
0.5 Hz	0.005	1	0.2
1 Hz	0.015	2.5	0.4
2 Hz	0.05	4	0.3
3 Hz	0.035	1.75	0.1
4 Hz	0.025	1.25	0.05
5 Hz	0.015	0.5	0.025

Table 3.4 The output which is measured in second floor

Frequency	(M7+M8)/2		
	Acc (g)	Vel (cm/sec)	Disp (cm)
0.5 Hz	0.007	1.3	0.2
1 Hz	0.017	2.7	0.5
2 Hz	0.06	5	0.3
3 Hz	0.05	2.5	0.12
4 Hz	0.04	2	0.075
5 Hz	0.03	1.5	0.04

Table 3.5 The output which is measured at top

Frequency	(M9+M10)/2		
	Acc (g)	Vel (cm/sec)	Disp (cm)
0.5 Hz	0.01	1.5	0.3
1 Hz	0.02	3	0.5
2 Hz	0.06	5	0.4
3 Hz	0.05	3	0.15
4 Hz	0.05	2.25	0.12
5 Hz	0.05	2	0.075

4. CONCLUSION

In the previous chapters the aseismic base isolation systems are introduced and a base isolation device so called Ball-N-Cone (BNC) is studied. The main characteristics of BNC system is the limitation of the acceleration transmitted to the structure by its cone angle.

Independent of the ground motion, the lateral force on the top of BNC is equal to cone slope times weight. In other words the output seismic force is physically limited, regardless of the seismic ground motion.

The results shows us the goal of decreasing the amount of shear force by its cone angle coming to the structure is well achieved by BNC system. The acceleration values in structure as low as 8% of g for each frequencies. In other words, the output acceleration magnitudes of structure is always less than 0.08 g that controls the restoring force. In addition, the amount of decrease in displacement can be controlled in the design stage of the isolator by increasing the cone angle.

In roller type of bearings, it is difficult to include friction and damping to control displacement. Using external dampers such as hysteretic damper would be more effective and cheaper solution.

REFERENCES

Anlı, E.C., 1999 *"Development of a Base Isolation Device for Protection of Museum Displays"*, Master of Science Thesis, Boğaziçi University.

Chopra, A, 2001, *"Dynamics of Structures"*, Prentice-Hall, New Jersey.

Coburn, A, Spence, R, 1992 *"Earthquake Protection"*, Wiley, Chichester.

Guerreiro, L., Azevedo, J., Muhr, A.; 2007 "Seismic Tests and Numerical Modeling of a Rolling-ball Isolation System", *Journal of Earthquake Engineering, 11:49-66*.

International Conference of Building Officials, "Uniform Building Code (UBC) – 1997", April 1997, http://www.ubc.com/

Kelly, M.J., 2004, " Seismic Isolation!, in Y. Bozorgnia, V.B. Vitelmo (eds), *"Earthquake Engineering from Engineering Seismology to Performance-Based Engineering"*, pp. 11-1 – 11-31, CRC Press, Florida

Önem, G., Tüzün, C., Durukal, E., Erdik, M; 2006 "Protection of Museum Items Against Earthquake Shaking By Low-Cost Base Isolation Devices", *4th World Conference on Structural Control and Monitoring*, International Association for Structural Control and Monitoring Paper No: 30, San Diego, California, USA

Ueda, S., Fujita T., Iiba M., Enomoto, T., 2005 "Study of Roller Type Isolation Device for Houses", *9th World Seminar on Seismic Isolation, Energy Dissipation and Active Vibration*, Kobe, 13 June-16 June 2005, Chapter 5-18, Kobe, Japan

Xiangyun, H., Xuehai, L., Quingmin, W., Dingguo, F., Quianfeng, Y., 2003 “Theoretical and Experimental Study on a Base Isolation System Using Roller Bearings”, *The Third International Conference on Earthquake Engineering*, Nanjing, 18 October-20 October 2003, Chapter 4-04, Nanjing, China

Yang, Y.B, Chang, K.C., Yau, J.D., 2003, “Base Isolation” in W. Chen, C. Scawthorn, “*Earthquake Engineering Handbook*”, pp. 17-1 – 17-30, CRC Press, Florida